Applied Thermal Engineering 280 (2025) 128401

Contents lists available at ScienceDirect

Applied Thermal Engineering

journal homepage: www.elsevier.com/locate/apthermeng

Research Paper

Techno-economic assessment of peak-shaving in coal-fired power plants with thermal energy storage systems based on steam accumulator

Qilong Xu [a], Shuai Wang [a,b], Kun Luo [a,b,*], Jianren Fan [a,b]

[a] State Key Laboratory of Clean Energy Utilization, Zhejiang University, Hangzhou 310027, China
[b] Shanghai Institute for Advanced Study of Zhejiang University, Shanghai 200120, China

ARTICLE INFO

Keywords:
Flexibility retrofit
Steam accumulator
Thermal energy storage
Peak-shaving performance analysis
Comprehensive performance evaluation
Economic assessment

ABSTRACT

Traditional coal-fired power plants (CFPPs) face significant challenges in rapidly responding to load fluctuations with the increasing integration of renewable energy into the grid, making flexibility enhancement a crucial issue for the power industry. Accordingly, this study developed a novel supercritical CFPP integrated with a steam accumulator (SA) system, designed to enhance peak shaving performance through efficient heat storage and release. First, an integrated model of a 600 MW supercritical CFPP coupled with a SA system is established and its reliability is validated. Second, an innovative AHP-EWM-TOPSIS comprehensive evaluation method is developed to optimize the scheme design under different steam inlet and outlet configurations, assess the peak-shaving performance of each integration scheme, compare their comprehensive performance scores, and identify the optimal solution. Finally, a detailed economic analysis of the proposed peak-shaving model is carried out, yielding key economic indicators for practical application. The results show that the highest performance score (0.884) is achieved when the main steam is selected as the storage source, while the optimal steam release location at the No. 1 extraction point yields the highest score (0.979). The proposed system demonstrates strong economic feasibility, achieving a net present value of 65.73 million CNY, a payback period of 2.51 years, and a levelized cost of electricity of 0.283 CNY/kWh, all outperforming conventional retrofits. These findings demonstrate that integrating steam accumulators provides a techno-economically viable pathway for enhancing CFPP flexibility, characterized by strong profitability, rapid revenue growth, and low costs.

1. Introduction

With the global energy transition and China's "peak carbon–carbon neutral" goal of continuous promotion, China is undergoing a critical energy transition, so in recent years, the installed capacity of renewable energy has shown a rapid growth trend. By 2024, China's installed renewable energy power generation capacity will reach 160 GW, of which the total installed capacity of wind and solar energy has exceeded 460 GW and 720 GW, respectively, becoming an important support for China's energy transition [1–3]. However, despite the remarkable progress made in the utilization of renewable energy, it is difficult to ensure a continuous and stable power supply due to its volatility and intermittency, which poses a great challenge to the scheduling and stable operation of the power system [4–6]. Therefore, to ensure the smooth operation of the energy supply, it is necessary to rely on a more flexible peak-shaving capacity [7,8]. Addressing challenges from large-scale access to renewable energy [9], especially improving the peak-shaving capacity and flexibility of the power system, has become a key issue for optimizing China's energy structure and the stable operation of the power system.

Coal-fired power plants (CFPPs) have a strong load regulation capability, which allows them to quickly adjust peaks and change loads in a short period according to the demand of the power grid, which is crucial for balancing the volatility of new energy sources and ensuring the stability of the power system [10,11]. Therefore, in power generation, traditional CFPPs still occupy an important position in China's power supply. Relying on traditional CFPPs for power production is still the backbone of the current power system. Especially in China, the CFPPs has a large scale and the economic benefits of long-term investment, and the direct elimination of these units will not only lead to substantial economic losses but also affect the stable operation of the power system [12,13]. However, in response to the fluctuating load after large-scale renewable energy grid connection, traditional CFPPs often cannot respond quickly to load changes and low efficiency in low load operation, resulting in energy waste and economic loss. Tradtional

* Corresponding author at: State Key Laboratory of Clean Energy Utilization, Zhejiang University, Hangzhou 310027, China.
E-mail address: zjulk@zju.edu.cn (K. Luo).

https://doi.org/10.1016/j.applthermaleng.2025.128401
Received 6 July 2025; Received in revised form 24 August 2025; Accepted 16 September 2025
Available online 19 September 2025

Nomenclature

Acronyms

CFPP	Coal-fired power plant
AHP	Analytic hierarchy process
TOSISI	Technique for order preference by similarity to an ideal solution
NPV	Net present value
LCOE	Levelized cost of investment

Subscripts

c	Energy storage process

List of symbols

$\Delta P_{c,t}$	peak-shaving capacities in the energy storage process, kW
$P_{c,t}$	power generated at time t, MW
$\xi_{c,t}$	peak-shaving depth at time t in the energy storage process, %
Q_t	energy storage load of the SA system during the energy storage process, kJ
P_{in}	the work done by the SA when the is storing steam, MW
q_c	the heat consumption rate in the energy storage process, kJ/kW
W_{net}	the net power generation by the plant, kWh
b_c	the coal consumption in the energy storage process, g/kWh
b_e	the lower calorific value of standard coal, kJ/kg
η_g	the pipeline efficiency, %
η_{c1}	the thermal efficiency, %
t_1	the start time of the energy storage process, s
t_3	the start times of the heat release process, s
$Q_{c,t}$	the heat loads output by the boiler at time t, kW
$E_{c,t}$	the fuel exergy at time t, kW
SA	Steam accumulator
EWM	Enropy weight method
CNY	Chinese yuan
SPBP	Static payback period
$\Delta P_{s,t}$	peak-shaving capacities in the energy release process, kW
$P_{s,t}$	power generated at time t, MW
$\xi_{s,t}$	peak-shaving depth at time t in the energy release process, %
Q_{in}	the total heat generated by the fuel entering the boiler, kJ
P_{out}	the work done by the SA when it is releasing steam, MW
q_s	the heat consumption rate in the energy release process, kJ/kW
Q_{re}	the heat consumption of the unit, kJ/h
b_s	the coal consumption in the energy release process, g/kWh
η_b	the boiler efficiency%
$\eta_{b,t}$	the thermal efficiency of the boiler at time t, %
η_{s1}	the thermal efficiency, %
t_2	the end time of the energy storage process, s
t_4	the end times of the heat release process, s
$Q_{s,t}$	the heat loads output by the boiler at time t, kW
$E_{s,t}$	the fuel exergy at time t, kW

CFPPs can no longer meet the peak-shaving demand of the power system, which seriously affects the stability of the power system [14–16].

As an important means for power systems to cope with load fluctuations and renewable energy volatility, flexibility retrofit technology is the basis for ensuring the stable operation of power grids [17,18]. With the transformation of the energy structure and the intelligent development of the power system, the flexibility retrofit of CFPPs has become an important issue to be solved in the power industry. Further flexibility retrofit and peak-shaving optimization of CFPPs not only help to improve the system's operational efficiency but also maximize the advantages of the existing units, effectively consume more renewable energy, and guarantee the smooth progress of energy transformation. 600 MW supercritical CFPPs, as one of the main power sources in China, still account for a high proportion of coal-fired power generation, especially in peak load shifting. It has unique advantages in terms of its high efficiency and low unit carbon emission and is widely used in various power plants [19,20]. Therefore, it is of great research significance and practical application value to study the measures to improve the peak-shaving capacity of 600 MW supercritical CFPPs and explore their optimization paths under the new energy situation [21–23].

Currently, there are several methods of peak-shaving transformation technology for CFPPs. The first one is to adopt the sliding pressure operation mode of the CFPP, which can adjust the steam parameters by changing the boiler's combustion load to realize the pocwer regulation. Still, it will lead to an increase in fuel consumption and a decrease in efficiency when operating at low loads [24,25]. The second is to optimize the combustion process by changing the combustion mode of the boiler or adopting advanced combustion control technology, which can improve the efficiency of the unit at low loads, but the retrofit cost is high and technically difficult [26]. The third is to introduce an energy storage technology. The traditional flexibility retrofit technology mostly relies on changing the combustion process or adjusting the unit operation mode to improve the efficiency at low load. Still, the retrofit complexity is higher [27]. Energy storage technology offers a promising solution. In the context of unstable renewable energy generation, by introducing energy storage technology, the energy storage system can store excess power and release it when the load demand is low, smoothing the load fluctuation of coal-fired units and improving the load regulation capability of the units [28,29].

Among various energy storage technologies, steam accumulators (SA) have unique advantages as devices suitable for thermal energy storage [30]. Compared with battery storage and other technologies, SA can efficiently utilize the steam system of the existing unit for energy storage and release, avoiding the loss of large-scale conversion of electric energy, with higher thermal efficiency, lower initial investment costs, and longer service life, making it more adaptable to the needs of CFPPs in terms of large-scale energy storage and regulation [31,32]. SA can store excess heat energy in the form of steam and quickly release it when needed, which can better match the operation mode of the CFPP, so that it can maintain stable operation efficiency during load fluctuations, which not only improves the peak-shaving capability but also reduces the energy waste in operation [33]. Moreover, SA can be directly coupled with the existing CFPPs in the retrofit process, which will not cause large changes to the original structure of the unit, the transformation process is relatively simple, avoiding complex engineering transformation and high investment costs [34]. Therefore, combining SA as a means of energy storage and CFPP peak-shaving has significant technical and economic advantages.

In recent years, steam accumulator (SA), as a mature energy storage technology, has been widely used in the industrial and electric power fields, aiming to enhance the flexibility of the power system and the capacity of renewable energy consumption. Murakoshi et al. [35] integrated SA into biomass power generation system, and found that the initial steam pressure directly affects the volume of the accumulator and the levelized cost of storage (LCOS), which verifies the feasibility of SA in improving the power generation flexibility. For solar direct steam power generation system, Ploquin et al [33] revealed the liquid level fluctuation mechanism of parallel SAs through CFD simulation and proposed that the liquid level difference can be reduced by optimizing the pressure drop of the pipeline network, thus enhancing the utilization

of energy storage capacity. In combined cycle power plants, González-Gómez et al. [36] proposed a "SA-concrete block" hybrid energy storage scheme, which utilizes the sensible heat storage properties of concrete blocks to superheat the steam, shortening the startup time of the system by 30 %, proving the synergistic advantages of multi-media energy storage. The synergistic advantage of multi-media energy storage is proved. For the deep peak-shaving scenario of coal-fired units, Ding et al [34] designed a bypass steam thermal storage system, and the dynamic simulation showed that it could achieve a fast power response of ±5 % at 40 % of rated load, with the peaking rate increased to 3 % Pe/min and the charge/discharge cycle efficiency of 63.6 %. In addition, Zhuang et al [37] introduced SA in an electric-steam coupled industrial system, which increased the renewable energy consumption rate by 23.81 % and reduced the operating cost by 11.39 % through isothermal linearization of the steam flow model and iterative optimization strategy. Li et al [32] verified the thermal economy of SA in mechanical vapor recompression (MVR) system, and experiments showed that its energy efficiency ratio (COP) reached 6.25, the startup time is 50 % shorter than that of traditional MVR, and the annual payback period is only 7 years. Ehtiwesh et al [38] constructed a dynamic model of a direct steam generation (DSG) solar system coupled with a SA for the Libyan hospital's electric power demand and verified its stable power supply capability under fluctuating light conditions through Simscape simulation.

From the above studies, it can be seen that SA, as an efficient heat storage technology, have demonstrated their potential for enhancing flexibility in biomass power generation, solar thermal systems, and industrial steam networks [39–41]. However, existing research has not yet addressed the engineering application bottlenecks of SA in deep peak shaving for large coal-fired units [42–44]. First, there is a lack of matching design between high-parameter steam (>10 MPa/566 °C) and SA for 600 MW-class supercritical coal-fired units—which account for the core proportion of China's coal-fired power generation capacity. Second, existing coal-fired peak shaving studies have primarily focused on combustion optimization or bypass steam modifications, lacking systematic solutions that integrate SA, particularly failing to elucidate the mechanisms by which steam storage/release pathways influence peak shaving performance. Third, economic analyses are limited to static investment estimates or theoretical models, without establishing a dynamic full-cycle benefit model to validate engineering feasibility. Therefore, subsequent research needs to explore innovative approaches that balance rapid response and economic feasibility in the peak shaving process of coal-fired power plants.

This study aims to address the technical and economic bottlenecks associated with deep peak shaving in large coal-fired power plants. The core objectives are: to develop a SA coupled system suitable for 600 MW supercritical units, enhancing peak shaving capacity by optimizing steam storage/release pathways; to establish a multi-dimensional technical–economic evaluation framework to quantify the comprehensive benefits of SA-based peak shaving; and to demonstrate the feasibility of engineering applications, providing a low-cost solution for flexibility upgrades in coal-fired power plants.

For this reason, this study pioneered the development of an integrated peak-shaving model for a 600 MW supercritical coal-fired power plant and SA, innovatively proposing a synergistic approach combining main steam storage and first-stage extraction steam release; Furthermore, an AHP-EWM-TOPSIS hybrid evaluation system was developed to comprehensively quantify the advantages and disadvantages of the scheme based on eight technical and economic indicators. Through economic analysis, the economic competitiveness of SA peak shaving was empirically demonstrated, providing an industrial-level solution for flexibility upgrades of coal-fired units.

2. Modeling and evaluation methods

2.1. Model construction of CFPP coupled with SA for peak-shaving

A SA is a steam storage vessel that stores and releases steam. In operation, a SA can use water or other fluids to store heat and release it when needed. Fig. 1 shows the structure of a typical SA. In the initial state, the SA contains liquid water at a certain pressure with a volume fraction of about 75 %, which is the recommended safety threshold for steam accumulator design.

During storage, the SA obtains high-temperature, high-pressure steam from the outside and stores it. The pressure inside the SA rises, and the storage process stops when the equipment pressure reaches the tolerance limit of the SA. In the high load demand conditions to open the steam release process, the release of saturated steam in the steam accumulator releases heat, resulting in a gradual decrease in the pressure in the SA, and the liquid water evaporates into steam. When the pressure reaches the initial pressure, the exhaust stops, and the exhaust process ends[33,38].

This study develops a steam storage and release model for a SA based on the following equilibrium equations to have a more detailed analysis of the variation of the parameters of the steam storage and release process in a SA [30,40], adopting the quasi-equilibrium assumption for vapor-liquid heat transfer between the water and the steam is sufficiently fast and that the water and the steam in the SA have the same temperature at the vessel pressure P [45,46]. The model is based on the following equilibrium equations.

(1) Mass balance equation for water and steam:

$$\frac{dm_w}{dt} = m_{w,in} - m_{w,out} + m_{e,w} - m_{c,s} \tag{1}$$

$$\frac{dm_s}{dt} = m_{s,in} - m_{s,out} + m_{c,s} - m_{e,w} \tag{2}$$

$$m_{e,w} = \rho_w \frac{1}{\tau_e} \frac{h_s - h_{s,sat}}{r} V_w, \quad m_{c,s} = \rho_w \frac{1}{\tau_c} \frac{h_{s,sat} - h_w}{r} V_s \tag{3}$$

where m_s is the mass of liquid water in the steam accumulator, kg; $m_{w,in}$, $m_{w,out}$ for the SA inlet, outlet water mass flow rate, kg/s; $m_{c,s}$ for the rate of SA, unit kg/s; $m_{e,w}$ for the rate of evaporation of water, kg/s; m_s for the mass of steam in the steam accumulator, kg; $m_{s,\ in}$, $m_{s,out}$ for the SA inlet, outlet steam mass flow rate, kg/s. τ_e is the relaxation time of the evaporation process, s; $h_{s,sat}$ for the enthalpy of saturated steam, kg/s. Respectively for the steam accumulator inlet and outlet steam mass flow rate, kg/s. τ_e is the relaxation time of the evaporation process, s; $h_{s,sat}$ is the enthalpy of saturated steam, kJ/kg; τ_c is the relaxation time of the condensation process, s; r is the latent heat of phase change, kJ/kg^{-1}.

(2) Energy balance equation for water and steam:

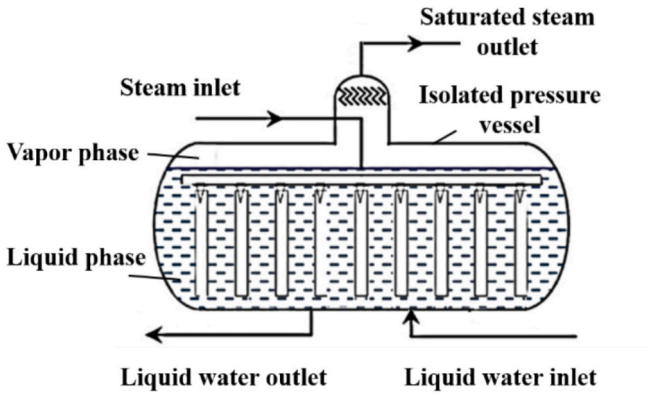

Fig. 1. Structure diagram of steam accumulator.

$$\frac{d(m_w h_w)}{dt} = m_{w,in}h_{w.in} - m_{w,out}h_{w,out} + (m_{e,w} - m_{c,s})h_{w,sat} + Q_{s,w} + V_w\frac{dP}{dt} \tag{4}$$

$$\frac{d(m_s h_s)}{dt} = m_{s,in}h_{s,in} - m_{s,out}h_{s,out} + (m_{c,s} - m_{e,w})h_{s,sat} - Q_{s,w} + V_s\frac{dP}{dt} \tag{5}$$

$$V_w + V_s = V_{SA}, \quad Q_{w,s} = (ha)_{s,w}V_w(T_2 - T_1) \tag{6}$$

where h_w is the specific enthalpy of saturated water in the SA, kJ/kg; $h_{w,in}$, $h_{w,out}$ are the specific enthalpy of saturated water at the inlet and outlet of the SA, kJ/kg; $h_{w,sat}$ is the specific enthalpy of saturated steam, kJ/kg; $Q_{s,w}$ is the heat exchanged between the liquid phase and the vapor phase, kW; V_w is the volume of saturated water, m^3; P is the pressure of the working medium in the accumulator, MPa; h_s is the specific enthalpy of steam in the SA, kJ/kg; $h_{s,in}$, $h_{s,out}$ are the specific enthalpy of the steam inlet and outlet of the accumulator, kJ/kg; V_s is the volume of steam in the SA, m^3; V_{SA} is the volume of the steam accumulator, m^3; ρ_w is the density of saturated water/(kg·m^{-3}); T_1, T_2 are the temperatures of saturated water and steam, K; $(ha)_{sw}$ is the product of the heat transfer coefficient between vapor and liquid and the concentration of vapor–liquid interfacial area, kW/(m^3·K).

The operation process of a CFPP coupled with a SA for peak-shaving is as follows: when the power load demand is low, the unit operates under low load conditions, with the initial load of the unit being 40 % THA (the lowest load that a CFPP can reach by relying on its load regulation). After introducing the SA, part of the steam generated from the boiler (the main steam selected for the initial scheme) is charged to the SA through the steam piping. The heat of the main steam is stored in the SA, the internal temperature and pressure of the SA continue to rise until it reaches the maximum pressure of the SA (10 MPa), the steam charging regulator valve closes, and the process storing the steam is completed. The process can be realized through the CFPP to reduce the load further. The load is further reduced. When the power load demand is high, the CFPP operates at full load 100 % THA condition, and the SA is in the state of steam release, the saturated steam under the corresponding pressure is released from the SA to the CFPP to the steam extraction (No. 1 high-pressure steam extraction is selected for the initial scheme), to reduce the amount of steam extraction, and to increase the amount of main steam used for the high-pressure cylinder of the turbine to do work. As the amount of steam released increases, the internal pressure of the SA decreases, and the released steam pressure decreases. When the pressure reaches the steam extraction pressure of CFPP, the steam release regulating valve closes, and the process of steam release is completed. The generating output can be improved through the steam release process, and the generating load of the CFPP can be increased.

During the storage and release process, since the SA absorbs superheated steam when storing it but releases saturated steam at the corresponding pressure when discharging, the liquid water in the SA will evaporate during discharge, and the stored steam will be less than the released steam, resulting in a loss of liquid water. Therefore, water must be refilled to restore the water level, maintain the initial level, and provide initial conditions for the next peaking process. It can be filled at the maximum feasible flow rate to ensure that the SA is restored to the initial level in the shortest possible time. Therefore, the replenishment rate should meet the boiler feedwater's minimum flow rate, estimated to be 180 t/h according to the boiler's operating procedure regarding the steam bypass system. Table 1 shows the internal parameters of the SA.

Ebsilon is selected for the process simulation software, capable of simulating the operation process under different operating conditions of the CFPP with high adaptability and detailed optimization and evaluation. The specific building process of the 600 MW CFPP is shown in the supplementary material. Table 2 shows the comparison between the simulated and designed values of the CFPP. By comparing it with the design value, it can be found that the error of the main parameters of the unit is small, with the maximum being only 1.2 %, which indicates that the model is reliable.The coupled peak-shaving model can be built based on the above peak-shaving process coupled SA and main initial parameters, as shown in Fig. 2.

Table 1
Initial parameters of the steam accumulator.

Parameter	Value
Initial pressure (MPa)	3.00
Internal volume (m^3)	500.00
Initial temperature (℃)	233.86
Internal enthalpy (kJ/kg)	1030.00
Heat transfer coefficient to the environment (W/(m^2·K))	10.00
Upper steam accumulator temperature limit (℃)	800.00
Upper steam accumulator pressure limit (MPa)	10.00
Thermal conductivity of insulation materials (W/(m^2·K))	0.40
Liquid volume fraction (%)	75.00

2.2. Scheme design of peak-shaving process

In order to further explore the heat storage and release capacity of the SA and optimize the peak-shaving process, the peak-shaving scheme will be optimally designed. According to the above peak-shaving process, the system efficiency and flexibility can be optimized by selecting different sources of steam as well as rationally arranging the release paths and steam extraction locations. In the process of steam storage, the SA inlet valve is open, and the steam release valve is closed, the SA can extract superheated steam from the CFPP in different locations for storage. Taking into account the steam temperature, pressure and other parameters of the unit in various locations, the main steam, reheat steam and high-pressure cylinder exhaust steam can be selected as the SA for storage. The parameters of the three kinds of steam are shown in Table 3, and the three different positions of steam correspond to Case S1, Case S2 and Case S3, respectively, and the specific arrangement of the three kinds of schemes is shown in Fig. 3.

In the process of steam release, optimizing the location of the SA's steam release port can accurately regulate the amount of steam released, reduce energy loss, improve the system's thermal energy utilization efficiency, and enhance the peak-shaving ability of the CFPP. Therefore, different peak-shaving schemes for the steam release process can be designed for different locations of the steam extraction ports. Due to the difference between main steam, low reheat steam, and high-pressure cylinder discharge pressure, it is necessary to match the location of the steam extraction port for the SA release according to the different steam storage sources. Table 4 shows the pressures at each extraction position for a CFPP at 100 % THA. It can be seen that when the main steam is selected, the pressure of the SA after the storage of steam is higher than the location of each extraction port, and the stored steam can be released to each extraction port.

To consider the compatibility of different steam storage and release locations and minimize losses, Table 5 shows the pressure differences between different steam storage sources and different steam release sources. It can be observed that due to the No. 5- No.8 section of the extraction of steam pressure being too low, the pressure difference between the main steam is large, which will produce large losses, requiring additional pressure reduction equipment, so it is necessary to avoid passing the main steam to these positions. Therefore, No. 1- No. 4 sections of the extraction steam port were selected as a steam release program, corresponding to the scheme Case R1-Case R4, as shown in Fig. 4. When reheat steam and high-pressure cylinder exhaust steam are selected as the source of steam storage, the storage pressure of the SA is lower than that of the No. 1- No. 3 sections of extraction, so the No. 4- No. 8 sections of extraction are selected as the steam release scheme, corresponding to Case R5- Case R9, are shown in Fig. 5.

Table 2
Comparison of simulated and design values for a 600 MW coal-fired plant under different operating conditions.

Parameter	Simulated value (100 %)	Design value (100 %)	Error (%)	Simulated value (40 %)	Design value (40 %)	Error (%)
Power generation capacity (MW)	602.60	600.00	0.43	240.54	240.0	0.26
Main steam temperature (℃)	566.50	566.00	0.1	566.3	566.0	0.05
Main steam pressure (MPa)	24.30	24.20	0.41	10.7	10.8	0.92
Main steam mass flow (t/h)	1800.60	1803.20	0.26	688.3	690.4	0.31
Reheat steam temperature (℃)	565.40	566.00	0.11	565.2	566.0	0.14
Reheat steam pressure (MPa)	3.96	3.94	0.51	1.60	1.61	0.63
Reheat steam mass flow (t/h)	1477.83	1483.34	0.37	582.72	584.35	0.27
Feedwater temperature (℃)	276.50	278.40	0.68	223.1	223.6	0.23

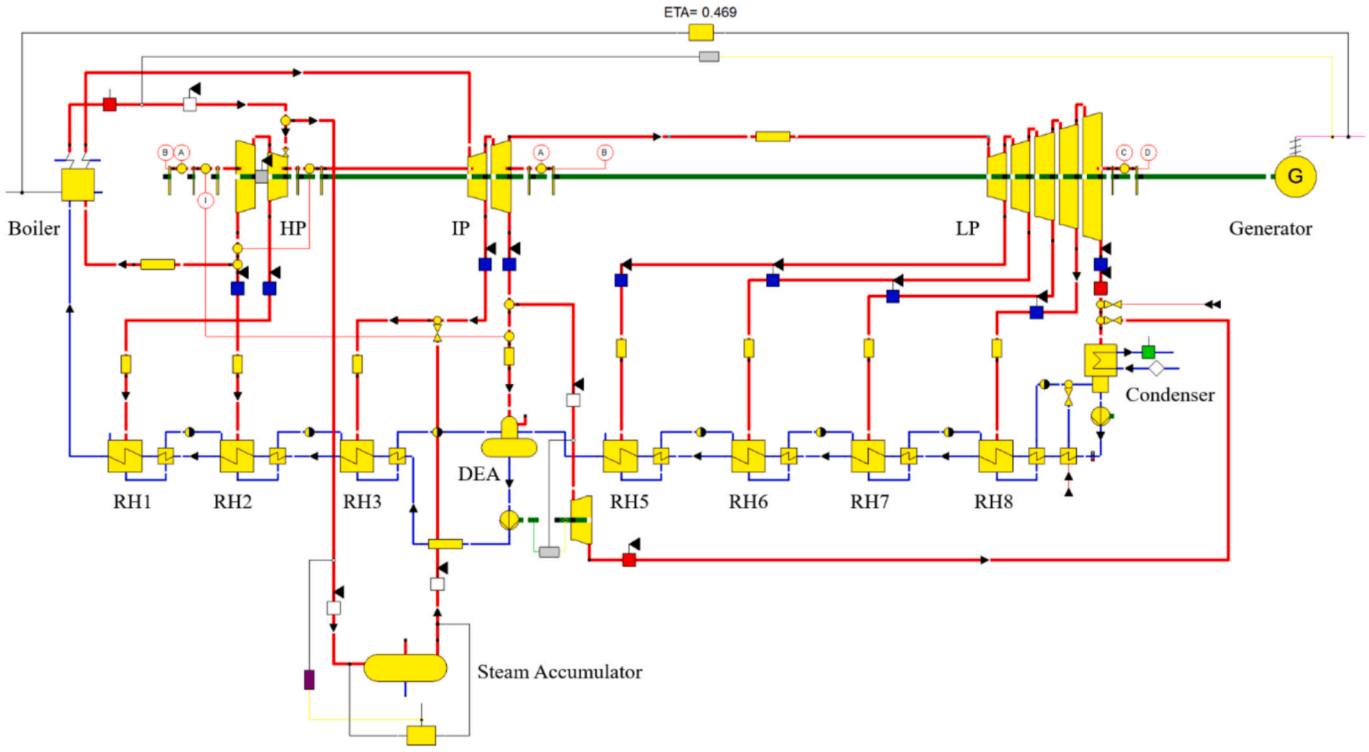

Fig. 2. Model diagram of a CFPP coupled SA for peak-shaving.

Table 3
Different outlet steam parameters of CFPP.

Parameters	Pressure (MPa)	Temperature (℃)
Main steam	10.50	566.00
Reheat steam	1.34	566.00
HP cylinder exhaust	1.38	321.20

2.3. Peak-shaving performance evaluation of coupling model

In order to study the impact of various steam storage and release schemes on the peak-shaving performance of the coupled model, this study selects peak-shaving capacity, peak-shaving depth, thermoelectric conversion efficiency, and round-trip efficiency as peak-shaving performance indicators. Additionally, this study selects heat consumption rate, coal consumption, thermal efficiency, and exergy efficiency as thermodynamic performance indicators for evaluating the SA energy storage system's steam storage and release process. Table 6 and Table 7 show the formulas for the peaking performance and thermodynamic performance indicators of the peaking model, respectively [47–49].

It can be seen that the performance evaluation indexes of the peak-shaving model are various. It is very subjective if only a single performance result is selected to evaluate the program's merits and demerits and is not comprehensible. Therefore, constructing a comprehensive evaluation system that integrates multi-dimensional indicators is necessary to obtain the peak-shaving system's comprehensive performance. Entropy Weight Method (EWM) – Analytic Hierarchy Process (AHP) – Technique for order preference by similarity to ideal solution (TOPSIS) evaluation method enhances the reliability of the evaluation by subjective and objective double empowerment. The comprehensive evaluation method considers subjective cognition and data objectivity, effectively avoids the single-assignment bias, and intuitively presents the program advantages and disadvantages through spatial distance measurement. The evaluation method can provide quantitative support for the decision-making of the peaking program of CFPPs.

Therefore, the AHP-EWM-TOPSIS evaluation method can be selected to evaluate the performance of the coupled model. The specific steps of the method are shown in Fig. 6, and the specific calculation formula is shown in the supplementary material [50–52].

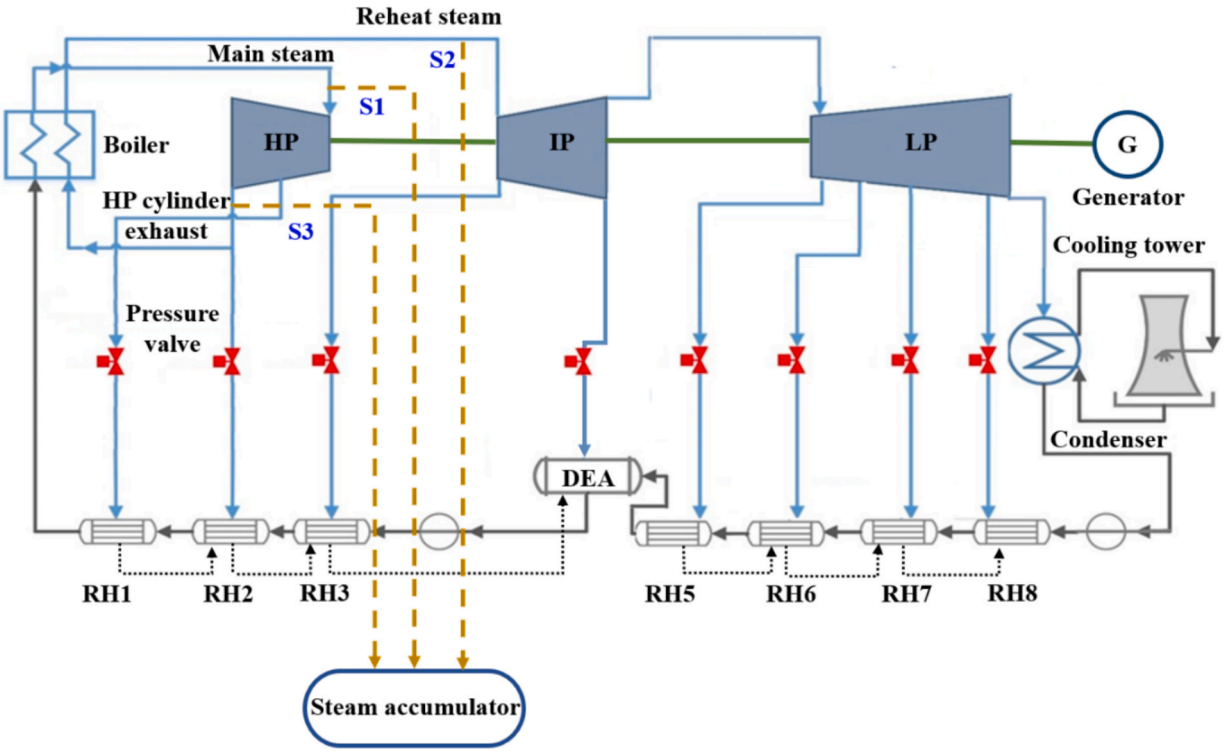

Fig. 3. Scheme design of steam storage of the coupled peak-shaving model.

Table 4
Parameters of each turbine extraction port under 100 % THA for 600 MW CFPP.

Parameters	Pressure (MPa)	Temperature (℃)	Saturation temperature (℃)	Overheating (℃)
No.1 Steam extraction	6.25	358.93	276.71	82.22
No.2 Steam extraction	4.08	309.14	251.32	57.82
No.3 Steam extraction	2.16	476.12	216.10	260.02
No.4 Steam extraction	1.07	370.65	182.95	187.7
No.5 Steam extraction	0.47	269.68	149.55	120.13
No.6 Steam extraction	0.13	140.84	107.14	33.7
No.7 Steam extraction	0.06	86.54	85.95	0.59
No.8 Steam extraction	0.02	60.52	60.06	0.46

Table 5
Pressure difference between steam extraction ports during steam storage and steam release from different sources.

Pressure difference (MPa)	Main steam	Reheat steam	HP cylinder exhaust
No.1 Steam extraction	4.25	−4.91	−4.87
No.2 Steam extraction	6.42	−2.74	−2.70
No.3 Steam extraction	8.34	−0.82	−0.78
No.4 Steam extraction	9.43	0.27	0.31
No.5 Steam extraction	10.03	0.87	0.91
No.6 Steam extraction	10.37	1.31	1.35
No.7 Steam extraction	10.44	1.28	1.32
No.8 Steam extraction	10.48	1.32	1.36

3. Technical-economic analysis and optimization of peak-shaving systems

3.1. Performance analysis and evaluation of different peak-shaving schemes for steam storage

In the process of steam storage, steam from different locations will be stored in the SA to reduce the unit's generating output and improve its peak-shaving capability. The choice of steam to be filled into the SA directly affects the storage process's heat density and system stability. The main steam is suitable for rapid filling. In contrast, the reheat steam and high-pressure cylinder exhaust steam can avoid overconsumption of the main steam and balance the energy distribution of the unit. The impact of different steam sources on the unit's peak shaving needs to be analyzed.

According to the above evaluation index calculation formula, you can obtain the results of the peak-shav performance of SA for each steam storage scheme, as shown in Fig. 7. At this time, the load heat of the three kinds of steam into the SA is the same, all of them are 70.00 MW. It can be found that when the main steam is used as the source of steam, the peak-shaving capacity and the peak-shaving depth are the highest, at 32.01 MW and 5.34 %, respectively. Case S2 has the worst peaking performance of 19.99 MW and 3.33 % because the reheat steam has the lowest pressure. When the high-pressure cylinder exhaust steam is used as the heat source, the thermal and exergy efficiency of the system is maximum, which is 38.22 % and 37.06 %, respectively. The reasons are that the heat loss and the exergy loss are minimized.

Through the calculation, the results of other important indexes of each scheme of the steam storage process are shown in Table 8. It can be found that Case S1 has the largest generation output of 208.83 MW, because of the optimal peak-shaving performance of Case S1, and the decrease in generation output is the largest compared to the initial CFPP. Similarly, the energy utilization factor of this scheme is also optimal, reaching 45.73 %. Since the thermal load of the steam storage process is constant, the larger the peak-shaving capacity of the steam storage

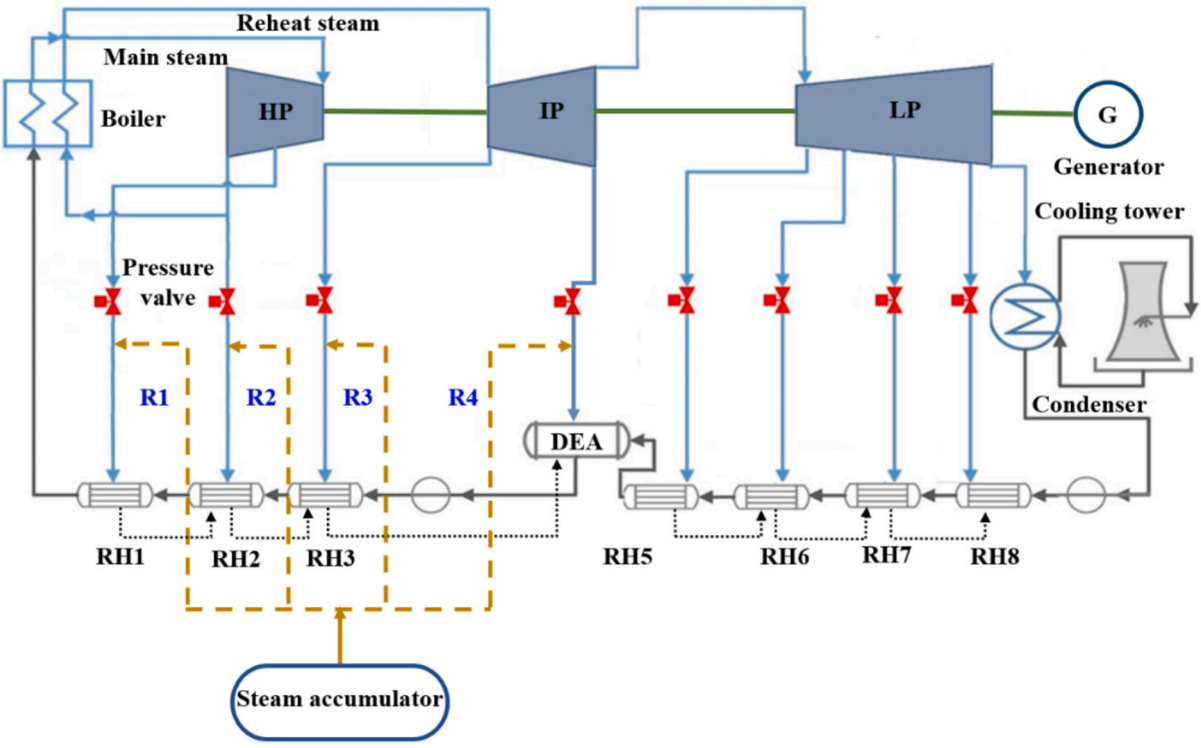

Fig. 4. Scheme design of steam release of the coupled peak-shaving model (main steam as the source of steam storage).

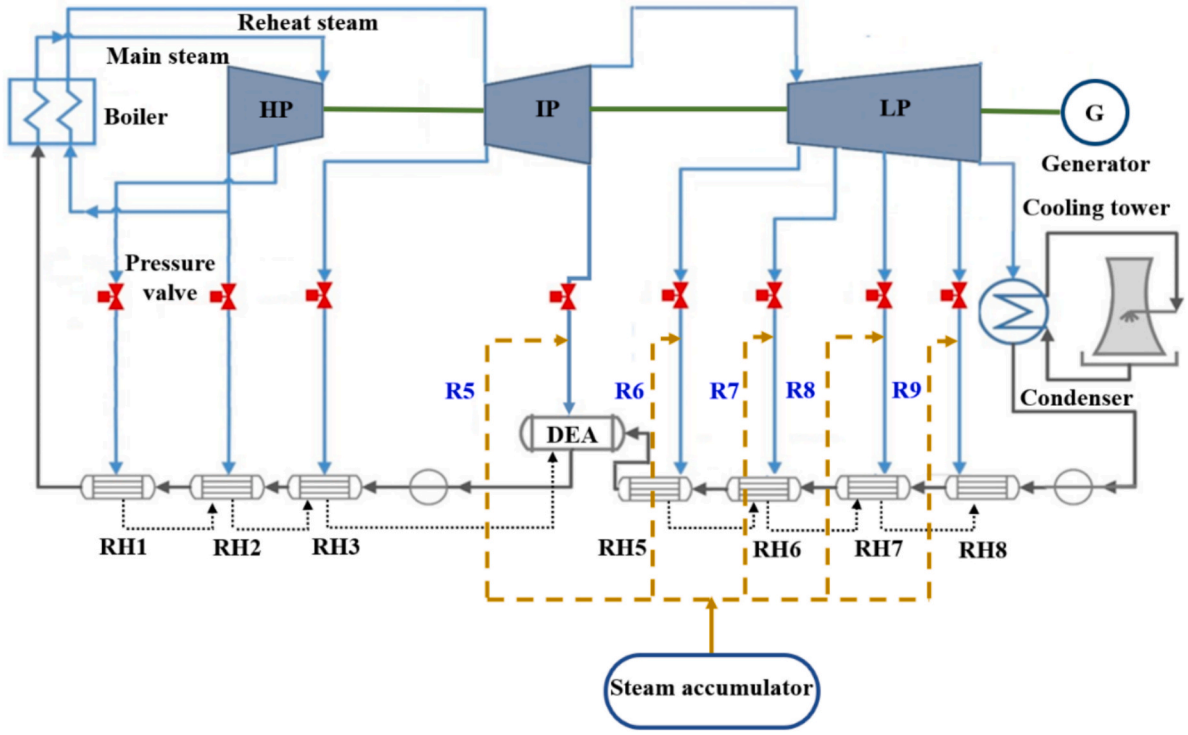

Fig. 5. Scheme design of steam release of the coupled peak-shaving model (reheat steam or high-pressure cylinder exhaust steam as the source of steam storage).

process, the larger the energy utilization factor of the scheme. However, Case S1 also has the largest coal consumption and heat consumption rate of 334.71 g/kWh and 9809.43 kJ/kWh, respectively, which is since Case S1 has the smallest power generation output. Hence, the energy consumption is greater with almost the same heat input from the CFPP.

At the same time, Table 8 also shows the environmental indicator – CO_2 emissions. The emissions of the three schemes are similar, with Case S2 having the lowest emissions at 840.08 gCO_2/kWh. However, compared to the CO_2 emissions of coal-fired units with 40 % THA without SA (838.59 gCO2/kWh), there is a significant increase, indicating that further reductions in unit load will increase CO_2 emissions.

To better evaluate the three steam storage schemes, the AHP-EWM-

Table 6
The calculation formula for flexibility performance index of energy storage and release processes.

Parameters	Energy storage process	Energy release process
Peak-shaving capacity (MW)	$\Delta P_{c,t} = P_0 - P_{c,t}$	$\Delta Ps,t = Ps,t - Pe$
Peak-shaving depth (%)	$\xi_{c,t} = \frac{\Delta P_{c,t}}{P_e} \times 100\%$	$\xi s,t = \frac{\Delta Ps,t}{Pe} \times 100\%$
Thermoelectric conversion efficiency (%)	$\eta_{c,t} = \frac{P_0 - P_{c,t}}{Q_t} \times 100\%$	$\eta_{c,t} = \frac{P_{s,t} - P_e}{Q_t} \times 100\%$
Round-trip efficiency (%)	$\eta_{rt} = \frac{P_{out}}{P_{in}} \times 100\%$	

Table 7
The calculation formula for thermodynamic performance index of energy storage and release processes.

Parameters	Energy storage process	Energy release process
Heat consumption rate (kJ/kWh)	$q_c = \frac{Q_{in}}{W_{net}}$	$q_s = \frac{Q_{in}}{W_{net}}$
Coal consumption (t/h)	$b_c = \frac{Q_{re}}{b_e \eta_b \eta_g} \times 1000$	$b_s = \frac{Q_{re}}{b_e \eta_b \eta_g} \times 1000$
Thermal efficiency (%)	$\eta_{c1} = \frac{\int_{t_1}^{t_2} (P_{c,t} + Q_{c,t})dt}{\int_{t_1}^{t_2} \left(\frac{Qc,t}{\eta b,t}\right)dt} \times 100\%$	$\eta_{s1} = \frac{\int_{t_3}^{t_4} P_{s,t}dt}{\int_{t_3}^{t_4} \left(\frac{Qs,t}{\eta b,t} + Q_{s,t}\right)dt} \times 100\%$
Exergy efficiency (%)	$\eta_{c2} = \frac{\int_{t_1}^{t_2} (P_{c,t} + E_{c,t})dt}{\int_{t_1}^{t_2} \left(\frac{Ec,t}{\eta b,t}\right)dt} \times 100\%$	$\eta_{s2} = \frac{\int_{t_3}^{t_4} P_{s,t}dt}{\int_{t_3}^{t_4} \left(\frac{Es,t}{\eta b,t} + E_{s,t}\right)dt} \times 100\%$
Carbon emissions (gCO_2/kWh)	$M_{CO_2} = \frac{b_{gd} C_{ar}}{100} \times \left(1 - \frac{A_{ar}}{100} \times \frac{A_c}{100}\right) \times \frac{44}{12}$	

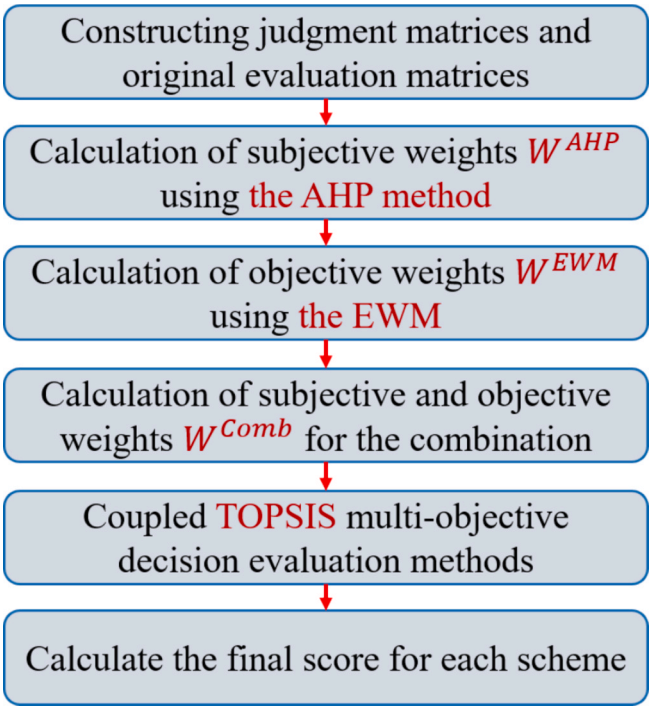

Fig. 6. Specific evaluation steps of the integrated evaluation system.

TOPSIS evaluation system is utilized to calculate the comprehensive scores for all the indicators of the steam storage schemes. The complete process of constructing the comprehensive evaluation system, as well as the specific calculation formulas for weights and comprehensive scores, are shown in Material 2 in the supplementary materials. Peak-shaving capacity, peak-shaving depth, thermal efficiency, exergy efficiency and energy utilization coefficient are selected as benefit-type indicators, respectively X1-X5; coal consumption and heat consumption rate of the unit are selected as cost-type indicators, respectively X6 and X7. Through the above evaluation system and the supplementary material calculation formula, the weights of the AHP method, EWM and the combined weights of the two methods, W^{Comb}, can be calculated, as shown in Fig. 8. It can be found that the combined weights of thermal efficiency and energy utilization coefficient are the largest, respectively, indicating that the advantages and disadvantages of the steam storage process in the peak-shaving model mainly depend on the thermal efficiency and energy utilization coefficient, while the combined weight of the heat consumption rate is the smallest.

By introducing the combined weights into the TOPSIS evaluation system, the ideal solution and integrated scores of each steam storage scheme can be obtained, as shown in Table 9 and Table 10. It can be found that Case S1 has the highest score of 0.884, and Case S2 has the lowest score of 0.102 in this comprehensive evaluation system, so the optimal scheme for the steam storage process in the peak-shaving model is Case S1. At this time, the main steam of the CFPP is used as a source of steam, which is passed into the SA for storage, and the optimal model diagram of the steam storage scheme is shown in Fig. 9.

3.2. Performance analysis and evaluation of different peak-shaving schemes for steam release

According to the above results, the main steam will be selected as the heat source for the steam storage process, and the steam release scheme of the peak-shaving model is shown in Fig. 4. At this time, the SA inlet valve is closed and the steam release valve is in the open state. The steam stored in the SA will be released to the steam extraction position of the CFPP to increase the turbine's ability to do work and the unit's power generation output. During the steam release process, The heat release load from SA is 70.00 MW, and the steam release parameters of each scheme are set as shown in Table 11.

According to the above evaluation index calculation formula, the performance results of each steam release scheme of the SA can be obtained, as shown in Fig. 10. It can be found that Case R1 has the largest peak-shaving capacity and peak-shaving depth, which are 18.17 MW and 3.03 %, respectively. As the pressure of the steam extraction section decreases, the peak-shaving performance of the coupled model decreases and reaches the minimum at Case R4, which are 13.70 MW and 2.29 %, respectively. As the steam released pressure in the SA and low-pressure steam extraction section pressure are more mismatched, lower steam availability will result. Due to this reason, the SA round-trip efficiency will also decrease with the lower pressure at the extraction port, which achieves the maximum at Case R1 with 56.76 %.

Through calculation, the results of other important indicators for each scheme of the steam release process are shown in Table 12. It can be found that Case R1 has the largest power generation output of 617.64 MW, the reason is that Case R1 has the optimal peaking performance, and the additional power generatLE ion output is the largest compared to the initial CFPP. Similarly, the energy utilization factor of this scheme is also optimal and reaches 25.82 %. The reason for this is that the heat load of steam released from the SA during the steam release process is constant, and the larger the peak-shaving capacity of the steam release process, the larger the energy utilization coefficient of the scheme. Case R4 has the largest coal consumption and heat dissipation rate, which are 274.31 g/kWh and 8039.20 kJ/kWh, respectively. The reason is that Case R4 has the smallest power generation output, so the energy consumption is larger in the case with almost the same heat input of the CFPP.

As shown in the table, CO_2 emissions are significantly reduced compared to the steam storage process, but the emissions from the four schemes are nearly identical, with Case R2 having the lowest emissions

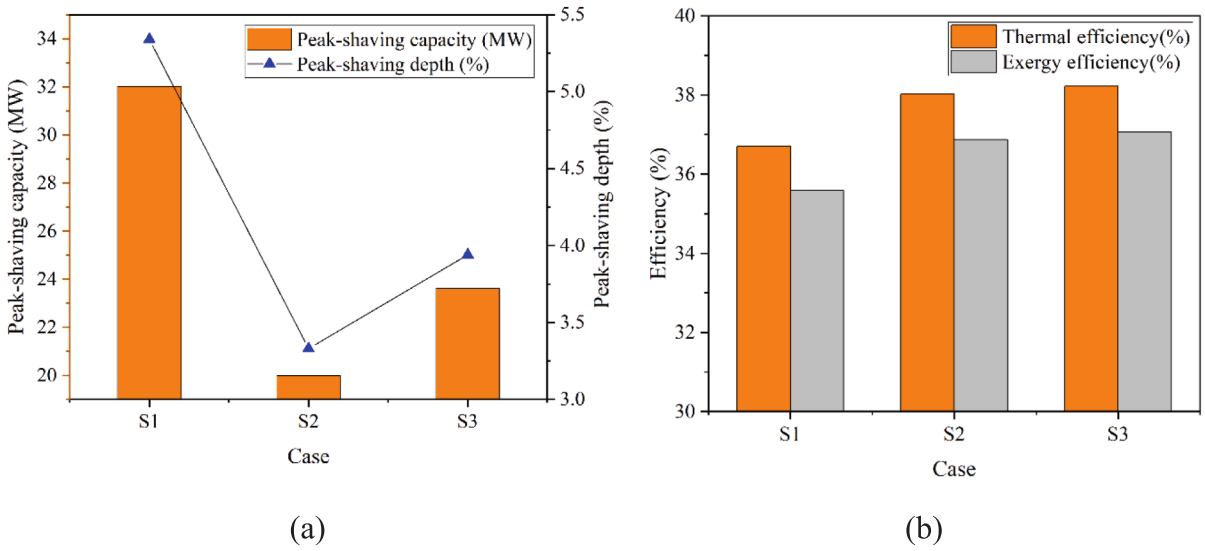

Fig. 7. Performance results of steam storage scheme: (a) peak-shaving performance, (b) thermodynamic performance.

Table 8
Results of the main indicators for different schemes of the steam storage process.

Parameter	Case S1	Case S2	Case S3
Charging mass flow (t/h)	71.15	69.61	82.45
Steam accumulator temperature (℃)	293.53	192.24	183.85
Steam accumulator pressure (MPa)	9.72	1.32	1.09
Internal enthalpy (kJ/kg)	1307.22	846.32	847.11
Liquid volume fraction (%)	70.50	31.60	31.90
Generating power (MW)	208.83	220.85	217.22
Energy utilization factor (%)	45.73	28.56	33.75
Coal consumption (g/kWh)	334.71	323.06	321.38
Heat consumption rate (kJ/kWh)	9809.43	9467.87	9418.81
Carbon emissions (gCO_2/kWh)	857.63	840.08	855.13

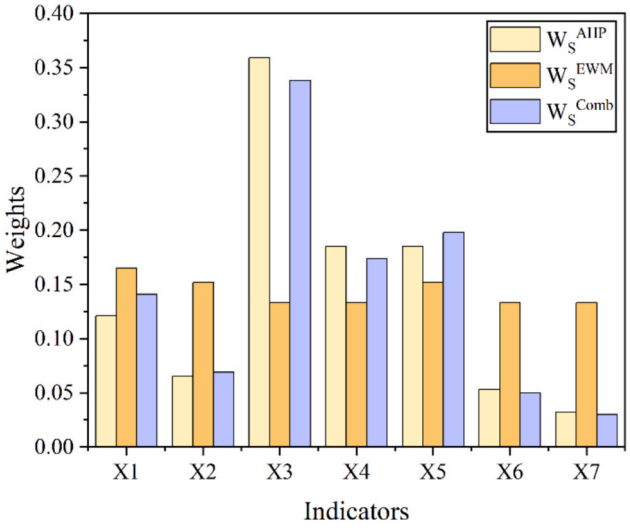

Fig. 8. Weights of indicators of the peak-shaving model in the energy storage process.

at 727.94 gCO_2/kWh. However, compared to the CO_2 emissions of a coal-fired power plant operating at 100 % THA without SA (802.16 gCO_2/kWh), there is a significant reduction, indicating that increasing the plant's load reduces CO_2 emissions. This also provides a reference for improving the environmental performance of the plant in the future.

In order to better judge the advantages and disadvantages of the four steam release schemes, the AHP-EWM-TOPSIS evaluation system is used to calculate the comprehensive scores of all the indicators of the steam release schemes. Based on the selection of the indicators of the steam storage process, the round-trip efficiency of the steam release scheme is added as the benefit-type indicator, which is X8. Through the above evaluation system, the weights of the AHP method, EWM, and the comprehensive weights combining the two methods can be calculated as shown in Fig. 11. It can be found that the comprehensive weights of the round-trip efficiency and the thermal efficiency are the largest at this time, respectively, indicating that the performance in the steam storage process mainly depends on these two indicators. While the integrated weights of coal consumption and heat consumption rate are the smallest.

Table 9
Calculation of positive and negative ideal solutions in different steam storage schemes.

Parameters	X1	X2	X3	X4	X5	X6	X7
Positive ideal solution	0.101	0.049	0.198	0.101	0.143	0.028	0.017
Negative ideal solution	0.063	0.031	0.019	0.098	0.089	0.030	0.018

Table 10
The combined score for three schemes of the peak-shaving model in the steam storage process.

Comprehensive score	Case S1	Case S2	Case S3
S_S	0.884	0.102	0.321

The integrated weights can be introduced into the TOPSIS evaluation system to get the ideal solution and integrated scores S_R of each scheme of the steam storage process, as shown in Table 13 and Table 14. From the above results, it can be found that Case R1 has the highest score in this comprehensive evaluation system, which is 0.979. Therefore, the optimal scheme for the peak-shaving model energy release process is Case R1, which is to pass the main steam stored in the SA to the No. 1 steam extraction position during the steam release process. The final obtained diagram of the peak-shaving model is shown in Fig. 12.

3.3. Economic analysis of the optimal peak-shaving model

When using SA technology to assist CFPP for peak-shaving, in

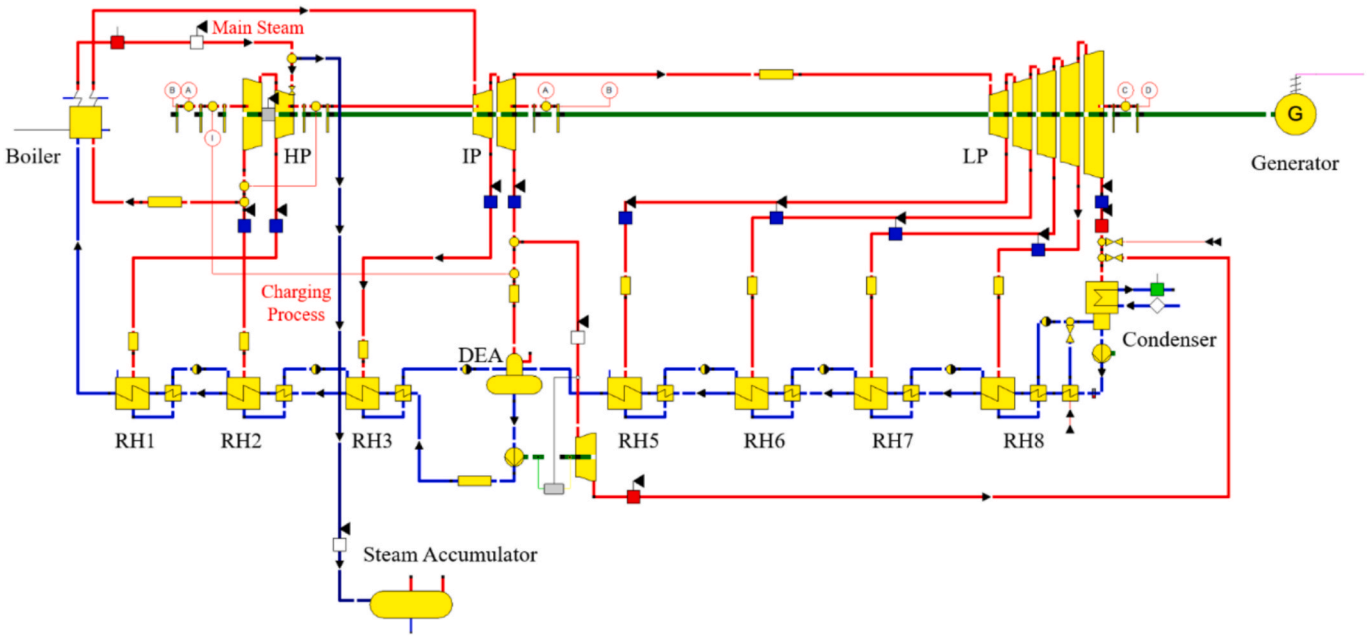

Fig. 9. Model diagram of the optimal steam storage scheme for the peak-shaving model.

Table 11
Parameter settings for each steam release scheme.

Parameters	Value	Parameters	Value
Coal consumption of the unit (40 %THA)	292.54	Coal consumption of the unit (100 %THA)	280.76
Steam release mass flow (t/h)	195.00	steam temperature of steam release (℃)	277.39
Steam release time (s)	3450	SA pressure after steam release (MPa)	6.17

addition to considering the technical indicators of the system, the specific cost of the peak-shaving model and the peak-shaving revenue are important influencing factors related to whether the peak-shaving technology can be put into practical application. Therefore, it is necessary to analyze the economic performance of the system, establish a quantitative evaluation system for the construction and operation costs and revenues of the system for the CFPP coupled with the SA energy storage technology, obtain the dynamic mapping relationship of the system cost-revenue, and construct a technical–economic evaluation model for the peak-shaving system to explore the economic feasibility of the peak-shaving technology [53,54].

3.3.1. *Economic analysis process based on peak-shaving model*

To study the economics of the steam storage and release process of SA in the peak-shaving process, the economic analysis of the peak-shaving model only considers the economics caused by the addition of the SA energy storage and release system, which mainly includes the calculation of the initial investment cost of the SA, the operation and maintenance (O&M) cost, and the revenues of the peak-shaving system.

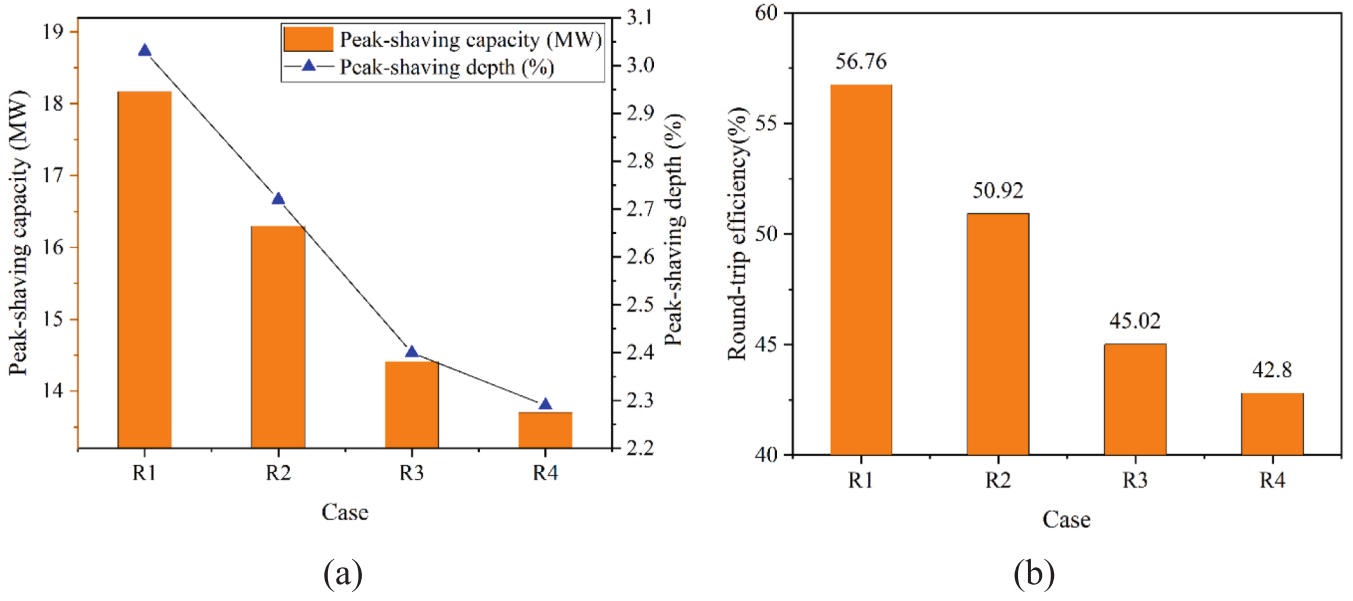

Fig. 10. Performance results of steam release scheme: (a) peak-shaving performance, (b) Round-trip efficiency.

Table 12
Results of the indicators for different schemes of the steam release process in SA.

Parameter	Case R1	Case R2	Case R3	Case R4
Generating power of power plant (MW)	617.64	615.76	613.88	613.17
Thermal efficiency (%)	44.90	44.91	44.88	44.78
Exergy efficiency (%)	43.53	43.54	43.51	43.42
Energy utilization factor (%)	25.82	23.15	20.47	19.46
Coal consumption (g/kWh)	273.58	273.52	273.71	274.31
Heat consumption rate (kJ/kWh)	8017.92	8016.15	8021.59	8039.20
Carbon emissions (gCO_2/kWh)	727.94	727.82	728.32	729.91

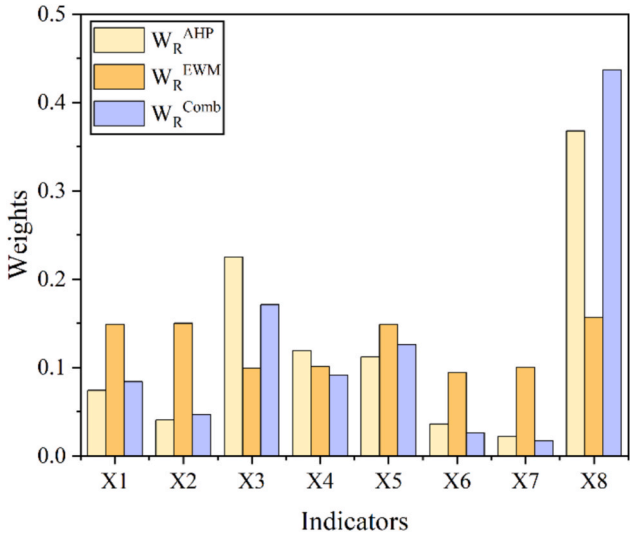

Fig. 11. Weights of indicators of the peak-shaving model in the steam release process.

The specific calculation steps are as follows [15]:

(1) Initial investment cost calculation. Initial equipment investment cost C_{inv} includes SA equipment cost C_{SA}, SA and piping installation cost C_{ins} and control system cost C_{con}.

$$C_{inv} = C_{SA} + C_{ins} + C_{\mathrm{con}}, \quad C_{SA} = V_{SA} \times P_{sa} \tag{7}$$

$$C_{ins} = \alpha \times C_{SA}, \quad C_{con} = \beta \times C_{SA} \tag{8}$$

where V_{SA} is the volume of the SA, P_{sa} is the equipment price per cubic meter of SA; α and β are the installation cost coefficients and control system cost coefficients, which were evaluated to be 0.25 and 0.20, respectively.

(2) Annual O&M costs. For the SA system, the annual operation and maintenance of the equipment are the main components of the system operating costs, which include the annual maintenance cost C_m, heat loss cost C_Q, water replenishment cost C_w, depreciation cost C_d, cyclic loading cost C_{cl}, and other costs (including potential downtime costs, grid connection reinforcement, and ancillary service requirements). The water replenishment cost is due to the SA needs to be replenished to the original level of the pre-peaking water replenishment costs after peak shaving each time. Depreciation cost refers to the effect of the value of the SA equipment spread over time.

$$C_{\mathrm{O\&M}} = C_m + C_Q + C_W + C_d + C_{cl} + C_o, \quad C_{\mathrm{m}} = \lambda \times C_{inv} \tag{9}$$

$$C_Q = \Delta Q_{\mathrm{loss}} \times P_{coal}, \quad \Delta Q_{\mathrm{loss}} = \eta_{\mathrm{loss}} \times V_{SA} \times \rho_s \times h_s \times a \times N_{peak} \tag{10}$$

$$C_w = \Delta V_w \times N_{\mathrm{peak}} \times a \times P_{\mathrm{w}}, \quad C_{\mathrm{d}} = \frac{C_{inv} - C_{sal}}{T} \tag{11}$$

where λ is the maintenance cost coefficient, taken as 0.04. ΔQ_{loss} is the annual heat loss, P_{coal} is the price of standard coal. η_{loss} is the daily heat loss rate of the SA, generally taken as 5 %, which is based on ASME PTC 4 and GB/T 39,288 standards, and takes into account the impact of enhanced insulation measures. ρ_s and h_s are the density and specific enthalpy of steam, respectively, and N_{peak} is the number of days of operation in a year. ΔV_w is the volume of water that is reduced in the SA at the end of each peak-shaving cycle, a is the number of peak-shaving cycles per day, and P_w is the price per cubic meter of water. C_{sal} is the salvage value, typically 5 % of the equipment cost. Considering the frequency of use of this peak-shaving model and the number of peak-shaving cycles, the service life T of the SA is taken as 20 years.

(3) Annual peak-shaving revenue. This part of the revenue includes annual peak-shaving compensation revenue R_{peak}, annual coal consumption revenue R_{coal} and electricity sales revenue R_{sale}. R_{peak} refers to the subsidized revenue gained from the participation of CFPPs in peak-shaving, which is an economic incentive set by the electricity market to encourage CFPPs to provide peak-shaving auxiliary services. R_{coal} is mainly generated by the increase of coal consumption in the peak-shaving process. R_{sale} refers to the indirect revenue gains realized through the peak-shaving process in the peak-to-valley tariff differential. Under the tariff mechanism, the price of electricity during peak hours is much higher than the price of electricity during trough hours.

$$R_{total} = R_{\mathrm{peak}} + R_{coal} + R_{sale}, \quad R_{peak} = \Delta P_{\mathrm{peak}} \times H_{peak} \times P_c \tag{12}$$

$$\Delta P_{\mathrm{peak}} = \frac{\Delta P_s \times t_s + \Delta P_r \times t_r}{t_s + t_r}, \quad H_{peak} = \mathrm{a} \times N_{peak} \times (t_s + t_r) \tag{13}$$

$$R_{coal} = R_{coal,s} + R_{coal,r}, \quad R_{coal,s} = \Delta b_s \times E_s \times P_{coal} \tag{14}$$

$$R_{coal,r} = \Delta b_r \times E_r \times P_{coal}, \quad R_{sale} = R_{\mathrm{sale},s} + R_{sale,r} - R_{sale,1} - R_{sale,2} \tag{15}$$

where ΔP_{peak} is the equivalent peak-shaving capacity of the storage and release process, H_{peak} is the number of annual peak-shaving hours, t_s and t_r are the single time lengths of the storage and release phases. p_c is the peak-shaving tariff subsidy, generally considered 0.35 CNY/kWh. Δb_s and Δb_r are the increase in coal consumption in the storage process and the decrease in coal consumption in the release process, respectively. E_s and E_r are the peak-shaving capacities of the storage and release processes, respectively. $R_{sale,s}$ and $R_{sale,r}$ are the annual generation revenues of the storage and release processes, respectively. $R_{sale,1}$ and $R_{sale,2}$ are the annual generation revenues of the unit under 40 % THA load and 100 % THA load before peak-shaving, respectively, and the duration is the same as that of the peak-shaving process. The electricity price is

Table 14
The combined score for four schemes of the peak-shaving model in the energy release process.

Comprehensive score	Case R1	Case R2	Case R3	Case R4
S_R	0.979	0.488	0.133	0.024

Table 13
Calculation of positive and negative ideal solutions in different steam release schemes.

Parameters	X1	X2	X3	X4	X5	X6	X7	X8
Positive ideal solution	0.048	0.027	0.085	0.046	0.073	0.013	0.009	0.261
Negative ideal solution	0.037	0.021	0.085	0.046	0.055	0.013	0.009	0.187

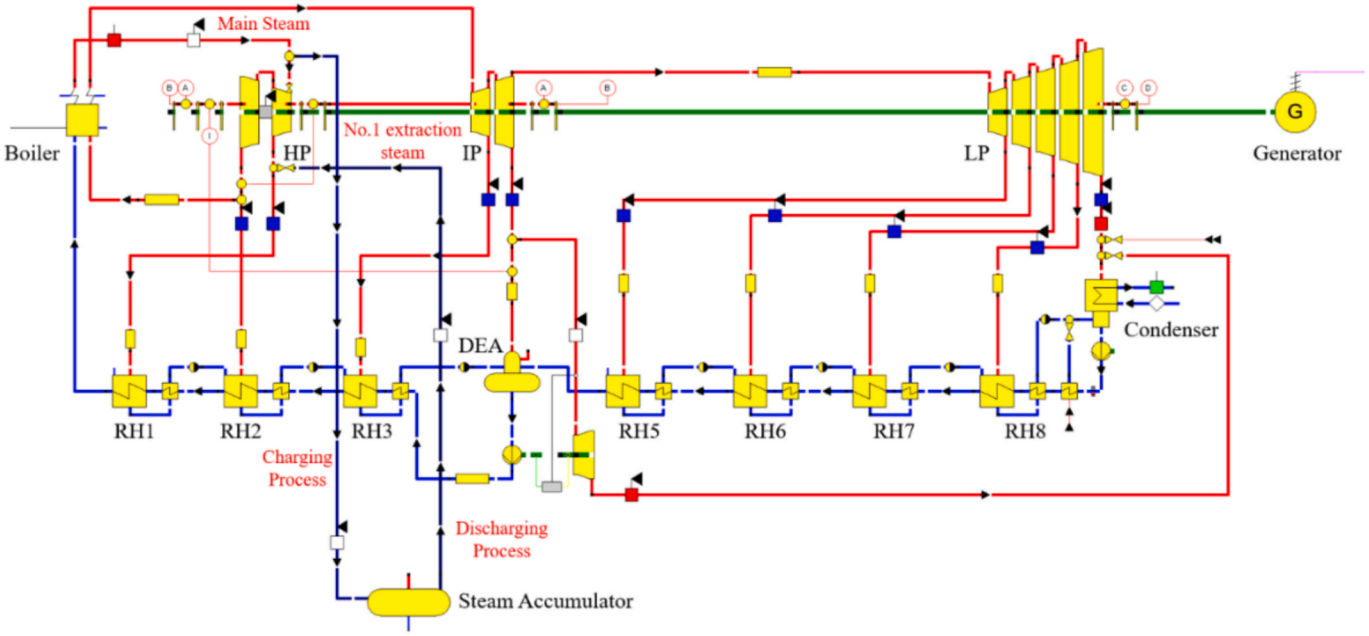

Fig. 12. Model diagram of optimal storage and release scheme for the peak-shaving model.

generally 0.8 CNY/kWh at peak time and 0.3 CNY/kWh at low valley time.

3.3.2. *Results of the economic analysis of the peak-shaving model*

By evaluating the performance of the peak-shaving model in the previous period, the parameters required for the economic analysis can be obtained, as shown in Table 15, and the unit price of SA equipment is determined based on the current market quotation for high-pressure vessels (10 MPa) and the pressure vessel cost guide. Combining the above formulas, the results of each index of the economic analysis of the peak-shaving model can be obtained, as shown in Table 16. It can be found that the equipment cost is 23.20 million CNY and annual peak-shaving revenue is 16.47 million CNY. The percentage of each part of the annual O&M cost is shown in Fig. 13, and the depreciation cost in the annual operating cost has the largest proportion, as high as 37.11 %. In the peak-shaving revenue, the coal consumption revenue is −3.19 million CNY, indicating the coal consumption will increase due to the introduction of the peak-shaving process, resulting in a reduction of the revenue, and the subsequent energy-saving optimization can be used to reduce the amount of coal consumption in the peak-shaving process and improve the economic efficiency of the peak-shaving model.

In order to comprehensively assess the economic feasibility of the peak-shaving model, the calculation of key economic indicators can be further carried out on the basis of the costs and revenues of the peak-shaving model. The key economic indicators mainly include net present value (NPV), static payback period (SPBP) and levelized cost of electricity (LCOE) [56,57]. Together, these three core indicators constitute a multi-dimensional assessment system for project feasibility. NPV quantifies the profitability of a project over its entire life cycle by discounting future cash flows, reflecting the true return under the time value of money, and a positive NPV indicates economic feasibility; SPBP focuses on the speed of the initial investment recovery, measuring risk in terms of time, with a short cycle implying a quick return of capital and an improved ability to withstand risk; The LCOE, from the perspective of kWh cost, apportions the total cost to each kWh of power generation, and directly benchmarks the market price of electricity or subsidy policy, revealing the cost competitiveness of the project.

Therefore, NPV provides a dynamic assessment of overall profitability, SPBP optimizes the capital turnover strategy, and LCOE ensures cost efficiency, which together provide a scientific basis for decision-makers to balance long-term profitability, short-term risk and cost control, and are the key decision-making cornerstones for the

Table 15
Essential parameters for economic analysis of peak-shaving model with SA [16,55].

Parameters	Value	Parameters	Value
V_{SA} (m^3)	500	N_{peak} (days)	300
P_{SA}(CNY/m^3)	32,000	a	3
P_{coal} (CNY/MJ)	0.024	P_w (CNY/t)	3
ρ_s (kg/m^3)	36.3	t_s (h)	1.058
h_s (kJ/kg)	2725	t_r (h)	0.958

Table 16
Results of economic analysis of peaking performance.

Parameters	Value	Parameters	Value
C_{inv} (million CNY)	23.20	C_{op} (million CNY/year)	2.40
R_{peak} (million CNY/year)	15.94	R_{coal} (million CNY/year)	−3.19
$R_{coal,s}$ (million CNY/year)	−5.87	R_{sale} (million CNY/year)	3.72
$R_{coal,r}$ (million CNY/year)	2.68	R_{total} (million CNY/year)	16.47

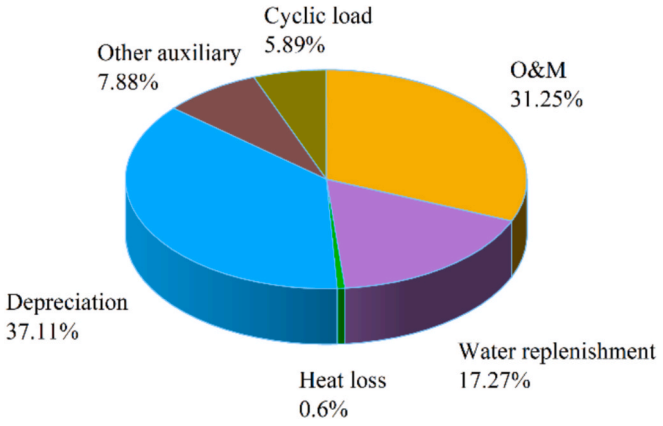

Fig. 13. Percentage of annual O&M costs of the peak-shaving system.

commercialization of peak-shaving technology. The specific calculation formula is as follows [58,59]:

$$NPV = -C_{inv} + \sum_{t=1}^{T} \frac{R_{total,t} - C_{O\&M,t}}{(1+r)^t} + \frac{C_{sal}}{(1+r)^T} \tag{16}$$

$$SPBP = \frac{C_{inv}}{R_{total} - C_{O\&M}} \tag{17}$$

$$LCOE_{SA} = \frac{C_{inv} + \sum_{t=1}^{T} C_{O\&M,t} \cdot (1+r)^{-t}}{\sum_{t=1}^{T} E_{peak,t} \cdot (1+r)^{-t}} \tag{18}$$

where r is the discount rate, typically 8 %, $R_{total,t}$ and $C_{O\&M,t}$ are the peak-shaving revenue and annual maintenance cost in year t, respectively, and $E_{peak,t}$ is the amount of electricity peak-shaving in year t.

The results of the key indicators can be obtained from the above formula, as shown in Table 17. It can be found that the NPV of the peak-shaving model couple SA is 65.73 million CNY, indicating that the peak-shaving model has strong profitability, and the SPBP of the system is only 2.51 years, indicating that the peak-shaving system will return to the capital and begin to generate revenue in a short period. Currently, the LCOE is only 0.283 CNY/kWh, which significantly reduces the cost of power generation relative to the conventional CFPPs. Therefore, it can be proved that the peak-shaving model of the coupled SA has a better economy, which is conducive to guiding the subsequent practical application of the peak-shaving technology.

The reliability of system economic assessments is highly dependent on the reasonableness of parameter settings related to costs, such as electricity sales costs, electricity purchase costs, investment costs, and the lifespan of energy storage systems. Therefore, to improve the reliability of economic analysis results, this study analyzed the impact of these cost parameters on key economic indicators (NPV, SPBP, LCOE), which investigate the changes in key indicators when the values of various influencing factors are reduced by 50 % or increased by 50 %. with the results shown in Fig. 14.

It was found that when NPV is the dependent variable, the trend of changes in electricity purchase prices is opposite to that of other variables and negatively correlated with net present value, indicating that an increase in electricity purchase prices will reduce the system's net present value. The rate of change in electricity sales prices is the highest, indicating that electricity sales prices have the greatest impact on net present value. When SPBP is the dependent variable, an increase in the energy storage system lifespan and selling price reduces the payback period, while an increase in investment costs and purchase price increases the payback period, with changes in the selling price having the greatest impact. When LCOE is the dependent variable, changes in the selling price do not affect the LCOE, while an increase in the purchase price increases the LCOE, and increases in the purchase price and energy storage system lifespan reduce the LCOE. These results will provide important support for further reducing the costs and improving the economic viability of coal-fired power plants coupled with SA models in subsequent studies.

3.3.3. Performance comparison of coal-fired power plant coupling SA with existing technologies and sensitivity analysis of key economic indicators

In order to more intuitively demonstrate the advantages of the coal-fired power plant coupled with the SA system in terms of response speed, renovation difficulty, and economic efficiency, this study compares this coupled system with other mainstream peak shaving technologies, focusing primarily on system performance and economic efficiency.

(1) The unique suitability of steam accumulators for coal-fired power plant retrofits

In order to further highlight the performance advantages of coal-fired power plants coupled with SA, this study compares the differences between the current mainstream peak shaving methods (such as molten salt thermal storage, compressed air energy storage, electrochemical energy storage, etc.) and the SA peak shaving method. The specific results are shown in Table 18. As can be seen from the above table, SA is irreplaceable in existing power plants with strict space restrictions and minimal host modifications (especially suitable for the coal-fired units studied in this paper, which are structurally complex and have limited space for modification).

(2) Economic comparison of different retrofit methods for coal-fired power plants

Using the economic analysis methods and detailed calculation formulas in the original text, we can compare the economic efficiency of different peak shaving methods [63,64]. The results are shown in Table 19. Through economic analysis, it can be seen that the steam storage method of steam accumulators has significant advantages in terms of unit investment, LCOE (CNY/kWh), and other indicators. Therefore, it can be proven that SA steam storage and release technology can provide more efficient and economical flexibility upgrades for existing coal-fired power plants, which is conducive to further promoting the large-scale consumption of new energy.

In summary, through the above detailed comparison, it can be seen that SA is more economical than mainstream energy storage technologies in short-term peak shaving scenarios, and the steam storage method of the steam accumulator does not require mid-term equipment replacement. But different methods have complementary performance. Further research should be conducted on hybrid peak shaving systems combining SA with molten salt energy storage and other methods to cover wide-range peak shaving demands.

Table 17
Crucial economic indicators of economic analysis of peak-shaving model.

Indicators	Value
NPV (10,000CNY)	6573.37
SPBP (years)	2.51
$LCOE_{SA}$(CNY/kWh)	0.283

4. Conclusion

To address the peak load regulation challenges faced by large-scale supercritical coal-fired power plants, this study conducts systematic research on the supercritical CFPP coupled with the SA system for peak-shaving, aiming to provide theoretical guidance for its efficient heat storage and peak-shaving. This research pioneers an integrated CFPP-SA model for the first time. innovatively designed multiple solutions and employed the AHP-EWM-TOPSIS comprehensive evaluation system to select the optimal solution. Through in-depth technical–economic joint analysis, this study has for the first time comprehensively demonstrated the prominent advantages of this technology in enhancing peak-shaving capacity (technical feasibility) and generating significant economic benefits (economic feasibility), establishing a methodological framework and optimization pathways for engineering applications.

For power plants with different steam parameters or grid requirements, the optimal combination of steam storage sources and release locations should be re-evaluated and determined based on their specific parameters and peak shaving objectives, using the design methodology and comprehensive evaluation system (AHP-EWM-TOPSIS) proposed in this paper. The methodology developed in this paper, which encompasses integrated design, performance evaluation, and economic analysis, provides a scalable framework for optimizing the peak-shaving application of steam accumulators (SA) in various types of coal-fired units. The following main conclusions are obtained:

(1) The optimal steam storage configuration utilizes main steam extraction, achieving maximum peak-shaving capacity (32.01 MW) and depth (5.34 %), outperforming reheat steam storage (19.99 MW, 3.33 %) and securing the highest comprehensive

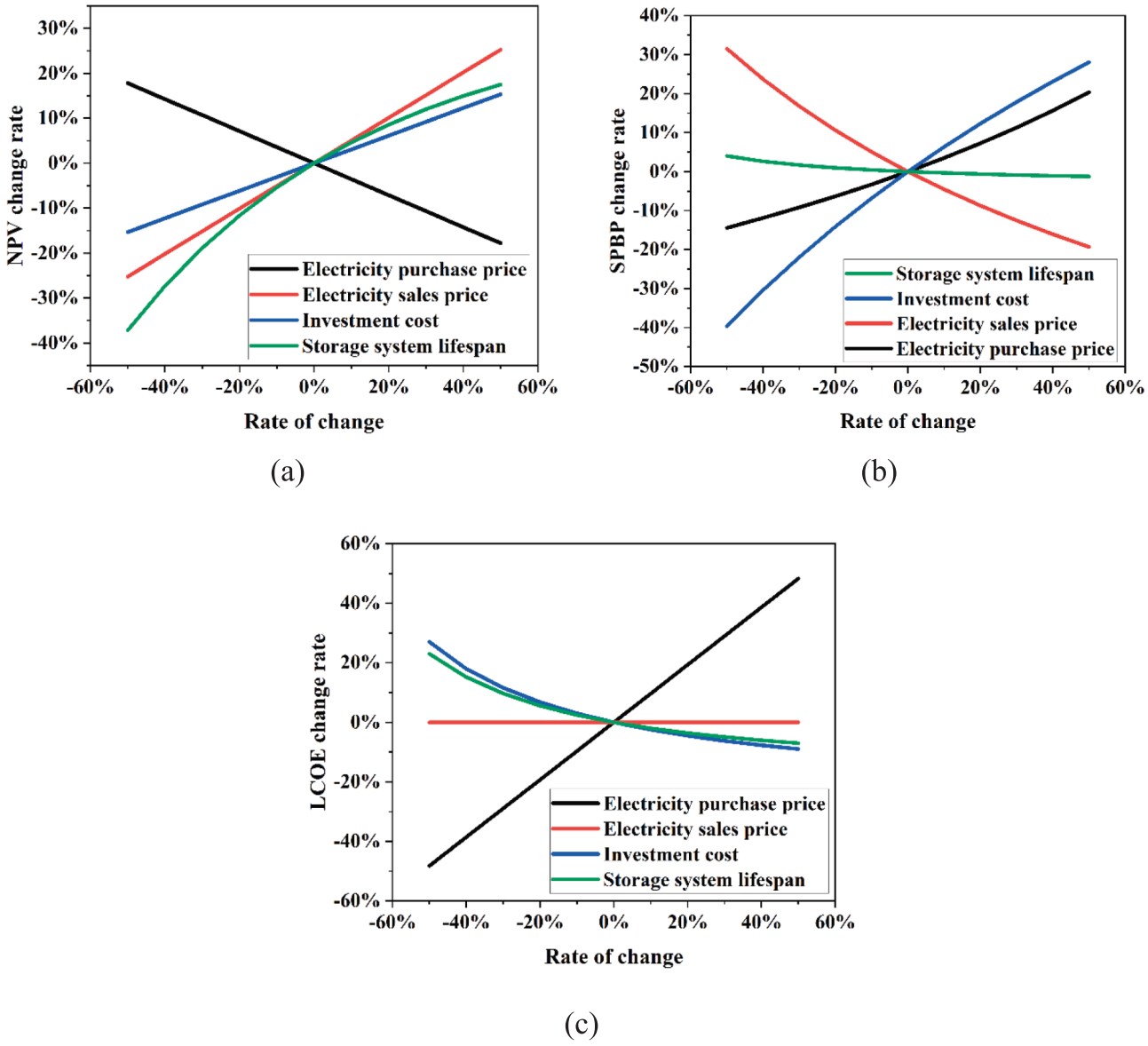

Fig. 14. The impact of changes in different parameters in the cost on key economic indicators: (a) NPV change rate, (b) SPBP change rate, (c) LCOE change rate.

Table 18
Comparison of the performance of the mainstream peak-shaving methods used in coal-fired power plants and this study's steam accumulator method.

Mainstream technology	Response speed	Main equipment renovation requirements	Space occupancy
Molten salt [16]	Minute level	A new heat exchange system is required	Very large (>5000 m^2)
Compressed air energy storage [60]	10–15 mins	Requires geological caverns/gas storage tanks	Very large
Electrochemical energy storage [61]	Millisecond level	Electrical connection renovation required	Medium
Steam accumulator	Second level	No need for complex modifications to the main equipment	In-situ installation (boiler room standby area)

Table 19
Comparison of the economic performance of the mainstream peak-shaving methods used in coal-fired power plants and this study's steam accumulator method.

Mainstream technology	Unit investment (ten thousand CNY/MW)	LCOE(yuan/kWh)	Cycling efficiency
Molten salt [16]	50–80	0.35–0.50	50–65 %
Compressed air energy storage [62]	80–120	0.40–0.70	60–70 %
Electrochemical energy storage [61]	75–90	0.58–0.80	85–90 %
Steam accumulator	37.5	0.283	73 %

evaluation score (0.884) in the AHP-EWM-TOPSIS system. For steam release, directing stored steam to the No. 1 extraction (Case R1) delivers superior performance with 18.17 MW capacity and 3.03 % depth - significantly exceeding lower-pressure extractions and attaining the top evaluation score (0.979). This confirms main steam storage coupled with No. 1 extraction release as the technically optimal solution.

(2) Economically, the system demonstrates robust viability with a total equipment cost of 23.20 million CNY and annual operational gains of 16.47 million CNY. Key metrics include a net present value of 65.78 million CNY, a remarkably short 2.51-year payback period, and a levelized cost of energy (LCOE) of 0.283 CNY/kWh, which has significant advantages over other flexible renovation methods. These results conclusively validate the model's technical feasibility, rapid profitability, and cost competitiveness for practical deployment.

Subsequent research will validate these findings via pilot-scale implementations. Typical power plants will be selected to deploy SA systems, and their dynamic performance will be tested under actual grid peak shaving requirements to provide empirical support for engineering promotion. Additionally, this study plans to extend the coal-fired power plant peak shaving model to the corresponding dynamic simulation platform (such as Simulink/APROS) in the future, quantify the dynamic characteristics of the SA system under grid frequency fluctuations (such as 0 %–100 % steam release valve response time and main steam pressure disturbance suppression capability), and analyze the phase compensation characteristics and grid adaptability of SA when participating in primary frequency regulation to improve the real-time response capability of the system.

CRediT authorship contribution statement

Qilong Xu: Writing – original draft, Validation, Software, Investigation. **Shuai Wang:** Writing – review & editing, Methodology. **Kun Luo:** Writing – review & editing, Supervision. **Jianren Fan:** Supervision, Conceptualization.

Declaration of competing interest

The authors declare that they have no known competing financial interests or personal relationships that could have appeared to influence the work reported in this paper.

Acknowledgments

We are grateful for the support from the National Natural Science Foundation of China (588020-X42405; 52576174), Fundamental Research Funds for the Central Universities (226-2024-00138; 2022ZFJH004), and Key Research and Development Program of Zhejiang Province (2025C01047).

Appendix A. Supplementary data

Supplementary data to this article can be found online at https://doi.org/10.1016/j.applthermaleng.2025.128401.

Data availability

Data will be made available on request.

References

[1] Q. Zeng, M. Hafeez, F. Sher, S. Ullah, Environmental higher education, formal finance, energy security risk, and renewable energy investment in China: an aggregate and disaggregate analysis, Renew. Energy 232 (2024) 121102, https://doi.org/10.1016/j.renene.2024.121102.
[2] D. Zhao, M. Sibt e-Ali, M. Omer Chaudhry, B. Ayub, M. Waqas, I. Ullah, Modeling the Nexus between geopolitical risk, oil price volatility and renewable energy investment; evidence from chinese listed firms, Renew. Energy 225 (2024) 120309, https://doi.org/10.1016/j.renene.2024.120309.
[3] X. Zhang, R. Zhang, C. Feng, Y. Wang, M. Zhao, X. Zhao, Decomposition analysis of renewable energy demand and coupling effect between renewable energy and energy demand: evidence from China, Renew. Energy 237 (2024) 121839, https://doi.org/10.1016/j.renene.2024.121839.
[4] C. Johnathon, A.P. Agalgaonkar, C. Planiden, J. Kennedy, A proposed hedge-based energy market model to manage renewable intermittency, Renew. Energy 207 (2023) 376–384, https://doi.org/10.1016/j.renene.2023.03.017.
[5] Z. Zhang, Z. Han, H. Hu, Y. Fan, J. Fan, Y. Shu, Self-adaptive system state optimization based on nonlinear affine transformation for renewable energy volatility, Renew. Energy 230 (2024) 120846, https://doi.org/10.1016/j.renene.2024.120846.
[6] I. Westphal, The effects of reducing renewable power intermittency through portfolio diversification, Renew. Sustain. Energy Rev. 197 (2024) 114415, https://doi.org/10.1016/j.rser.2024.114415.
[7] J. Xu, Q. Zhang, N. Ye, Z. Zhang, X. Wu, H. Fan, A review on flexible peak shaving development of coal-fired boilers in China under the carbon peak and carbon neutrality goals, Therm. Sci. Eng. Prog. 55 (2024) 103004, https://doi.org/10.1016/j.tsep.2024.103004.
[8] G. Hou, T. Huang, H. Jiang, H. Cao, T. Zhang, J. Zhang, et al., A flexible and deep peak shaving scheme for combined heat and power plant under full operating conditions, Energy 299 (2024) 131402, https://doi.org/10.1016/j.energy.2024.131402.
[9] B. Liu, T. Liu, S. Liao, H. Wang, X. Jin, Short-term operation of cascade hydropower system sharing flexibility via high voltage direct current lines for multiple grids peak shaving, Renew. Energy 213 (2023) 11–29, https://doi.org/10.1016/j.renene.2023.05.095.
[10] H. Zheng, J. Xu, J. Xie, G. Liu, Regulation of reheating temperatures for sCO2 coal-fired power plant to improve the peak regulation depth, Energy 322 (2025) 135485, https://doi.org/10.1016/j.energy.2025.135485.
[11] G. Zhang, K. Jiang, Q. Wang, Q. Zhang, J. Chen, J. Xu, et al., Dynamic performance and control strategy of steam generation system for ultra-rapid steam production in coal-fired power plant, Energy 320 (2025) 135368, https://doi.org/10.1016/j.energy.2025.135368.
[12] Y. Fu, L. Wang, M. Liu, J. Wang, J. Yan, Performance analysis of coal-fired power plants integrated with carbon capture system under load-cycling operation conditions, Energy 276 (2023) 127532, https://doi.org/10.1016/j.energy.2023.127532.
[13] L. Miao, M. Liu, K. Zhang, Y. Zhao, J. Yan, Energy, exergy, and economic analyses on coal-fired power plants integrated with the power-to-heat thermal energy storage system, Energy 284 (2023) 129236, https://doi.org/10.1016/j.energy.2023.129236.
[14] Y. Wu, Z. Wang, C. Shi, X. Jin, Z. Xu, A novel data-driven approach for coal-fired boiler under deep peak shaving to predict and optimize NOx emission and heat exchange performance, Energy 304 (2024) 132106, https://doi.org/10.1016/j.energy.2024.132106.
[15] X. Han, P. He, Z. Liu, C. Sun, X. Wang, Thermodynamic performance and economic analysis of coupled a liquid carbon dioxide energy storage system in a coal-fired power plant, J. Storage Mater. 99 (2024) 113201, https://doi.org/10.1016/j.est.2024.113201.
[16] Q. Zhang, J. Dong, H. Chen, F. Feng, G. Xu, X. Wang, et al., Dynamic characteristics and economic analysis of a coal-fired power plant integrated with molten salt thermal energy storage for improving peaking capacity, Energy 290 (2024) 130132, https://doi.org/10.1016/j.energy.2023.130132.
[17] Z. Mu, Y. Lv, K. Jiang, Q. Zhang, Q. Wang, F. Fang, et al., A dynamic nonlinear model for controller design of flue gas-molten salt heat exchanger in flexibility retrofit coal-fired unit, J. Storage Mater. 101 (2024) 113897, https://doi.org/10.1016/j.est.2024.113897.
[18] C. Zhuang, R. Choudhary, A. Mavrogianni, Uncertainty-based optimal energy retrofit methodology for building heat electrification with enhanced energy flexibility and climate adaptability, Appl. Energy 341 (2023) 121111, https://doi.org/10.1016/j.apenergy.2023.121111.
[19] M.U. Yousuf, M.A. Siddiqui, M. Kumar, M. Umair, Life cycle assessment of lignite-fueled ultra-supercritical coal-fired power plant with evaluation of solar energy integration, Fuel 385 (2025) 134079, https://doi.org/10.1016/j.fuel.2024.134079.
[20] K. Liu, L. Wang, W. Bai, D. Che, Comparative study on dynamic characteristics of 600 MW supercritical coal-fired boilers using CO2 and water as working fluids, Energy 314 (2025) 134296, https://doi.org/10.1016/j.energy.2024.134296.
[21] X. Liu, L. Zhang, K. Jin, X. Xue, H. Zhou, Integration model and performance analysis of coupled thermal energy storage and ejector flexibility retrofit for 600 MW thermal power units, J. Clean. Prod. 428 (2023) 139337, https://doi.org/10.1016/j.jclepro.2023.139337.
[22] C. Wang, Y. Zhao, M. Liu, Y. Qiao, D. Chong, J. Yan, Peak shaving operational optimization of supercritical coal-fired power plants by revising control strategy for water-fuel ratio, Appl. Energy 216 (2018) 212–223, https://doi.org/10.1016/j.apenergy.2018.02.039.
[23] Z. Liu, C. Wang, M. Fan, Z. Wang, F. Fang, M. Liu, et al., Investigation on the allowable load ramping-up rate and wet-to-dry conversion time of a 660 MW supercritical coal-fired power plant with deep peak-shaving work conditions, Energy 314 (2025) 134200, https://doi.org/10.1016/j.energy.2024.134200.
[24] Y. Fu, Y. Huang, H. Xin, M. Liu, L. Wang, J. Yan, The pressure sliding operation strategy of the carbon capture system integrated within a coal-fired power plant: Influence factors and energy saving potentials, Energy 307 (2024) 132737, https://doi.org/10.1016/j.energy.2024.132737.
[25] G. Ge, X. Cai, H. Sun, Y. Zhang, H. Wang, R. Li, Optimization design of an adiabatic compressed air energy storage system with sliding pressure operation and packed bed thermal energy storage based on a one-dimensional loss model, Energ. Conver. Manage. 328 (2025) 119626, https://doi.org/10.1016/j.enconman.2025.119626.

[26] Y. Cui, K. Jiang, H. Wei, X. Du, A steam combination extraction thermal energy storage scheme in boiler side for coal-fired power plant flexibility retrofit, J. Storage Mater. 98 (2024) 113038, https://doi.org/10.1016/j.est.2024.113038.
[27] T. Banerjee, J. Bravo, N. Sarunac, M. D'Agostini, C. Romero, Sustainable energy storage solutions for coal-fired power plants: a comparative study on the integration of liquid air energy storage and hydrogen energy storage systems, Energ. Conver. Manage. 310 (2024) 118473, https://doi.org/10.1016/j.enconman.2024.118473.
[28] D. Wang, Z. Sun, Q. Xu, R. Tian, W. Han, J. Shen, Thermodynamic modeling and analysis of a Carnot battery system integrating calcium looping thermochemical energy storage with coal-fired power plant, Energ. Conver. Manage. 318 (2024) 118888, https://doi.org/10.1016/j.enconman.2024.118888.
[29] F. Wu, Y. Liu, R. Gao, Challenges and opportunities of energy storage technology in abandoned coal mines: a systematic review, J. Storage Mater. 83 (2024) 110613, https://doi.org/10.1016/j.est.2024.110613.
[30] Z. Li, X. Zhang, Dynamics characteristics of steam accumulator using phase change materials with different operation modes: a case study, J. Storage Mater. 115 (2025) 115938, https://doi.org/10.1016/j.est.2025.115938.
[31] A. Guan, S. Zhou, W. Gu, J. Chen, H. Lv, Y. Fang, et al., Enhancing stability of electric-steam integrated energy systems by integrating steam accumulator, Appl. Energy 364 (2024) 123049, https://doi.org/10.1016/j.apenergy.2024.123049.
[32] J. Li, Z. Si, D. Han, Z. Hang, Thermo-economic performance enhancement in batch evaporation process via mechanical vapor recompression system coupled with steam accumulator, Desalination 532 (2022) 115735, https://doi.org/10.1016/j.desal.2022.115735.
[33] M. Ploquin, S. Mer, A. Toutant, F. Roget, CFD investigation of level fluctuations in steam accumulators as thermal storage: a direct steam generation application, Sol. Energy 245 (2022) 11–18, https://doi.org/10.1016/j.solener.2022.08.048.
[34] H. Ding, S. Ding, Q. Tan, C. Zhang, Q. Fang, T. Yang, Improving power ramp rate of a coal-fired power plant by a bypass steam accumulator, Heliyon 10 (2024) e32412, https://doi.org/10.1016/j.heliyon.2024.e32412.
[35] R. Murakoshi, C. Fushimi, Integration of a steam accumulator with a biomass power-generation system for flexible energy storage and discharge: effect of the initial steam pressure on the steam discharge profile and levelized cost of storage, J. Storage Mater. 55 (2022) 105586, https://doi.org/10.1016/j.est.2022.105586.
[36] P.A. González-Gómez, M. Laporte-Azcué, M. Fernández-Torrijos, D. Santana, Hybrid storage solution steam-accumulator combined to concrete-block to save energy during startups of combined cycles, Energ. Conver. Manage. 253 (2022) 115168, https://doi.org/10.1016/j.enconman.2021.115168.
[37] Z. Wennan, Z. Suyang, C. Jinyi, G. Wei, Operation optimization of electricity-steam coupled industrial energy system considering steam accumulator, Energy 289 (2024).
[38] A. Ehtiwesh, C. Kutlu, Y. Su, S. Riffat, Modelling and performance evaluation of a direct steam generation solar power system coupled with steam accumulator to meet electricity demands for a hospital under typical climate conditions in Libya, Renew. Energy 206 (2023) 795–807, https://doi.org/10.1016/j.renene.2023.02.075.
[39] T.K. Ibrahim, M.M. Rahman, Parametric simulation of triple-pressure reheat combined cycle: A case study, Adv. Sci. Lett. 13 (1) (2012) 263–268.
[40] M.K. Mohammed, W.H. Al Doori, A.H. Jassim, T.K. Ibrahim, A.T. Al-Sammarraie, Energy and exergy analysis of the steam power plant based on effect the numbers of feed water heater, Journal of Advanced Research in Fluid Mechanics and Thermal Sciences 56 (2) (2019) 211–222.
[41] K.I. Hamada, M.N. Mohammed, R.R. Jasim, T.K. Ibrahim, Energy and exergy analyses of a combined power plant based on natural gas combustion, Tikrit Journal of Engineering Sciences 30 (3) (2023) 17–26. https://doi.org/10.25130/tjes.30.3.3.
[42] O.J. Khaleel, F.B. Ismail, T.K. Ibrahim, S.H. bin Abu Hassan, Energy and exergy analysis of the steam power plants: A comprehensive review on the Classification, Development, Improvements, and configurations, Ain Shams Engineering Journal 13 (3) (2022) 101640, https://doi.org/10.1016/j.asej.2021.11.009.
[43] O.J. Khaleel, Developing an analytical model to predict the energy and exergy based performances of a coal-fired thermal power plant, Case Stud. Therm. Eng. (2021), https://doi.org/10.1016/j.csite.2021.101519.
[44] L.T. Shireef, Influence of operating parameters on the performance of combined cycle based on exergy analysis, Case Stud. Therm. Eng. (2022), https://doi.org/10.1016/j.csite.2022.102506.
[45] M. Ilic, V.D. Stevanovic, M.M. Petrovic, S. Milivojevic, Numerical investigations of steam accumulator dynamics: Assessment of computational models, J. Storage Mater. 96 (2024) 112633, https://doi.org/10.1016/j.est.2024.112633.
[46] V.D. Stevanovic, B. Maslovaric, S. Prica, Dynamics of steam accumulation, Appl. Therm. Eng. 37 (2012) 73–79, https://doi.org/10.1016/j.applthermaleng.2012.01.007.
[47] L. Gong, Y. Li, Y. Wang, Y. Zhang, Study on the peak shaving performance of coupled system of compressed air energy storage and coal-fired power plant, J. Storage Mater. 107 (2025) 114954, https://doi.org/10.1016/j.est.2024.114954.
[48] B. Sun, Y. Zhao, S. Zhang, J. Zhou, J. Liu, P. Zhang, et al., Thermodynamic performance analysis of steam power plants during deep peak shaving processes: Integrating a novel top turbine system in ultra-low loads, Energy 315 (2025) 134425, https://doi.org/10.1016/j.energy.2025.134425.
[49] Z. Chen, C. Su, H. Zhan, L. Chen, W. Wang, H. Zhang, et al., Thermodynamic and economic analyses of nuclear power plant integrating with seawater desalination and hydrogen production for peak shaving, Int. J. Hydrogen Energy 82 (2024) 1372–1388, https://doi.org/10.1016/j.ijhydene.2024.08.055.
[50] X. Li, Y. Peng, Y. Guo, W. Wang, X. Song, An integrated simulation and AHP-entropy-based NR-TOPSIS method for automated container terminal layout planning, Expert Syst. Appl. 225 (2023) 120197, https://doi.org/10.1016/j.eswa.2023.120197.
[51] T. Zhou, T. Lin, R. Cheng, G. Wang, B. Jiang, An integrated approach for spatio-temporal assessment and attribution of water resources carrying capacity: Incorporating AHP, TOPSIS, and lorenz asymmetry coefficient methods, J. Hydrol. 650 (2025) 132536, https://doi.org/10.1016/j.jhydrol.2024.132536.
[52] A.M. Al-Abadi, A.M. Handhal, M.A. Abdulhasan, W.L. Ali, J.J. Hassan, A.H. Al Aboodi, Optimal siting of large photovoltaic solar farms at Basrah governorate, Southern Iraq using hybrid GIS- based Entropy-TOPSIS and AHP-TOPSIS models, Renew. Energy 241 (2025) 122308, https://doi.org/10.1016/j.renene.2024.122308.
[53] X. Shi, Q. He, Y. Liu, X. An, Q. Zhang, D. Du, Thermodynamic and techno-economic analysis of a novel compressed air energy storage system coupled with coal-fired power unit, Energy 292 (2024) 130591, https://doi.org/10.1016/j.energy.2024.130591.
[54] J. Zhang, R. Liu, G. Zhang, W. Zhang, J. Wang, F. Wang, Techno-economic analysis and life cycle assessment of coal-to-aromatics process with integration of renewable energy-based hydrogen generation technology, J. Clean. Prod. 434 (2024) 139841, https://doi.org/10.1016/j.jclepro.2023.139841.
[55] R. Bartnik, Z. Buryn, A. Hnydiuk-Stefan, Thermodynamic and economic analysis of effect of heat accumulator volume on the specific cost of heat production in the gas-steam CHP plant, Energy 230 (2021) 120828.
[56] Y. Chen, Y. Wu, X. Liu, J. Ma, D. Liu, X. Chen, D. Liu, Energy, exergy and economic (3E) analysis of a novel integration process based on coal-fired power plant with CO2 capture & storage, CO2 refrigeration, and waste heat recovery, Energy 299 (2024) 131443, https://doi.org/10.1016/j.energy.2024.131443.
[57] W. Liao, X. Zhang, H. Ke, S. Zhang, J. Shao, H. Yang, et al., The techno-economic-environmental analysis of a pilot-scale positive pressure biomass gasification coupled with coal-fired power generation system, J. Clean. Prod. 402 (2023) 136793, https://doi.org/10.1016/j.jclepro.2023.136793.
[58] Y. Wang, H. Chen, T. Li, P. Pan, R. Zhai, G. Xu, et al., Thermo-economic analysis of a waste-to-energy assisted carbon capture system for a coal-fired power plant, Appl. Therm. Eng. 229 (2023) 120594, https://doi.org/10.1016/j.applthermaleng.2023.120594.
[59] M. Cossutta, S. Pholboon, J. McKechnie, M. Sumner, Techno-economic and environmental analysis of community energy management for peak shaving, Energ. Conver. Manage. 251 (2022) 114900, https://doi.org/10.1016/j.enconman.2021.114900.
[60] L. Zhang, J. Cui, Y. Zhang, T. Yang, J. Li, W. Gao, Performance analysis of a compressed air energy storage system integrated into a coal-fired power plant, Energ. Conver. Manage. 225 (2020) 113446, https://doi.org/10.1016/j.enconman.2020.113446.
[61] M.S. Mohtasim, B.K. Das, Advancement of biocarbon materials in sustainable thermal and electrochemical energy storage with future outlooks, Renewable and Sustainable Energy Reviews 218 (2025) 115779, https://doi.org/10.1016/j.rser.2025.115779.
[62] R. Cao, W. Li, X. Cong, Y. Duan, Energy, exergy and economic (3E) analysis and multi-objective optimization of a combined cycle power system integrating compressed air energy storage and high-temperature thermal energy storage, Appl. Therm. Eng. 238 (2024) 122077, https://doi.org/10.1016/j.applthermaleng.2023.122077.
[63] Q. Xu, S. Wang, K. Luo, et al., Energy-saving retrofit and thermal economy optimization of peak-shaving for coal-fired power plants utilizing molten salt thermal storage[J], Applied Thermal Engineering (2025) 128229.
[64] Q. Xu, X. Li, J. Yu, et al., Optimization of parameters and thermodynamics of gasification process for enhanced CO2 capture in an IGCC system[J], Energy 304 (2024) 131853, https://doi.org/10.1016/j.energy.2024.131853.